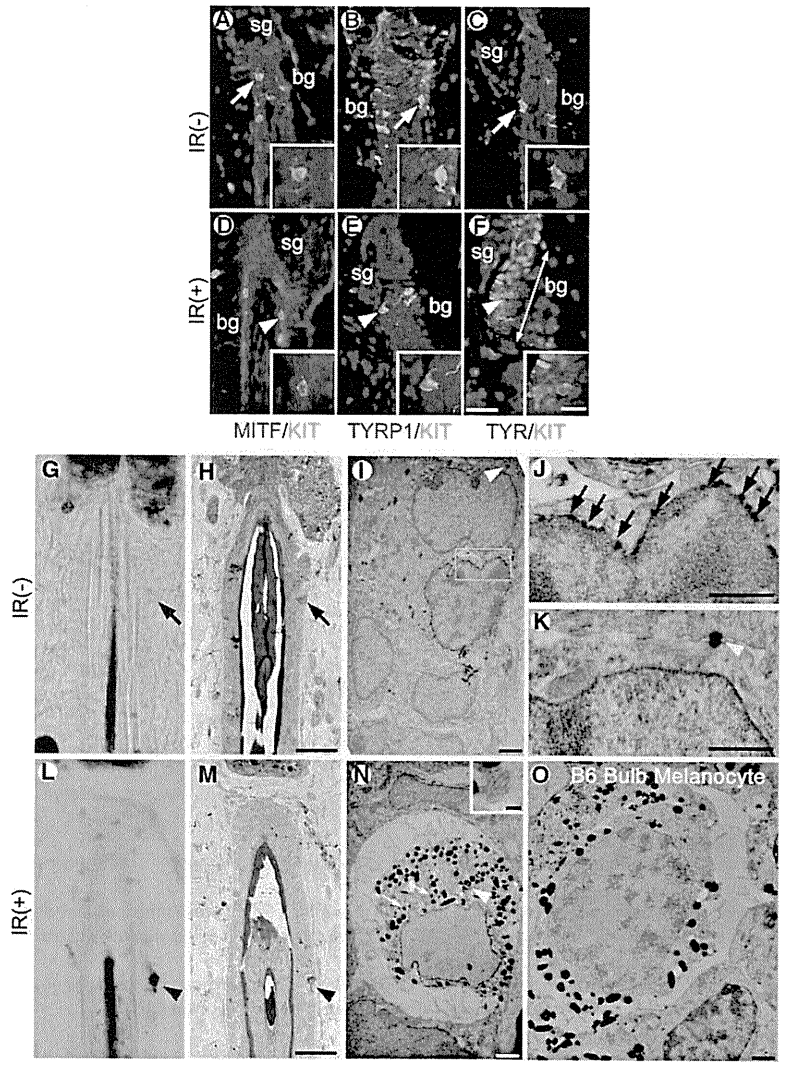

Figure 5. Ectopic Differentiation of MSCs in the Niche with Melanosome Maturation by Activation of the Canonical Differentiation Program

(A–F) Immunohistochemical changes of KIT$^+$ cells in the bulge areas of anagen IV follicles. Expression of MITF (red) and melanogenic enzymes, TYRP1 and TYR (red), is retained in KIT$^+$ cells (green) after IR (D–F, arrowheads) but not in control (A–C, arrows). The insets show magnified views of the KIT$^+$ cells (A–C and D–F).

(G–O) TEM analysis of Dct-lacZ$^+$ cells in the hair follicle bulge areas of *Dct-lacZ* transgenic mice after IR. (G and L) lacZ-stained hair follicles embedded in epoxy resin before sectioning. (H and M) Semi-thin sections with toluidine blue staining of (G) and (L), respectively. (I and N) TEMs of the lacZ$^+$ cells shown in (G) and (L). lacZ$^+$ cells were identified by electron-dense precipitates of X-gal reaction products in the nuclear membrane (I and N, black arrows in J). (J and K) Magnified images of the lacZ$^+$ cells (J) and a lacZ$^-$ keratinocyte (K). A desmosome-like structure (white arrowhead) was found at the cell-cell junction of lacZ$^-$ cells (K). Compared to the control (I), the irradiated lacZ$^+$ EPM contains abundant mature melanosomes (N). The inset in (N) shows a magnified image of a stage II melanosome indicated with the white arrowhead. (O) TEM of a differentiated melanocyte in the bulb of hair follicles of wild-type (C57BL6/J) mice without IR as a positive control. Abbreviations: bg, bulge; sg, sebaceous gland. Scale bars represent 25 μm in (F), (H), and (M), 10 μm in the inset of (F), 1 μm in (I), (N), and (O), 100 nm in the inset of (N), and 500 nm in (J) and (K).

due to pheomelanin (red/yellow pigment) synthesis by hair follicle melanocytes in homozygotes (Figure S9A). Total melanin content and mature melanosome formation are significantly reduced in *Mc1r*$^{e/e}$ melanocytes both in vivo and in vitro (D'Orazio et al., 2006; Hirobe et al., 2007), which indicates that MSH-MC1R signaling promotes melanocyte maturation. To determine whether the IR-induced ectopic differentiation of MSCs and/or the eventual loss of EPMs in the niche depend on MSH-MC1R signaling, extension mutant mice (*Mc1r*$^{e/e}$) and wild-type control mice (*Mc1r*$^{E/E}$) were treated with different doses of IR (Figure S9C–S9L). Melanocytes with dendritic morphology were induced by IR at doses of 5 Gy or 7 Gy but not at less than 3 Gy both in the *Mc1r*$^{E/E}$ controls and in *Mc1r*$^{e/e}$ mice (Figures S9C–S9G). Although IR failed to induce visible pigmentation in MSCs in the absence of functional MC1R, a small number of follicles that contain small amounts of pheomelanin in the bulge of *Mc1r*$^{e/e}$ follicles were clearly detectable (Figures S9M–S9O). These findings indicate that the IR-induced differentiation of MSCs in the niche consists of two steps: a MC1R signaling-independent maturation (as seen in *Mc1r*$^{e/e}$ mutants) and a MC1R signaling-dependent advanced step required for further melanosome maturation and increased melanosome formation. Furthermore, EPMs disappeared from the niche at anagen VI, which resulted in hair graying in subsequent hair cycles in both *Mc1r*$^{e/e}$ and *Mc1r*$^{E/E}$ mice (Figures S9R–S9V, 2N, 2O, 2S, 2T, and S4). These data show that the eventual elimination of EPMs from the niche and the resultant hair graying do not depend on MSH-MC1R signaling or on melanocytic maturation level. This suggests that DDR signaling upstream of MC1R-mediated melanogenic processes determines the eventual fate of damaged stem cells in the niche.

ATM Deficiency Sensitizes MSCs to Ectopic Differentiation in the Niche

By irradiating mice deficient in ATM, we tested whether MSCs undergo differentiation in the niche in response to DNA damage. *Atm*$^{-/-}$ mice showed dramatic hair graying even with 3 Gy IR while *Atm*$^{+/+}$ mice did not gray at all with the same dose of IR (Figure 6A). Consistent with the macroscopic changes, 3 Gy IR induced the appearance of EPMs in the bulge area in *Atm*$^{-/-}$ but not in wild-type controls (Figures 6H–6K). These EPMs induced in *Atm*$^{-/-}$ mice by 3 Gy IR (Figure 6J) were indistinguishable from those induced in wild-type mice by 5 Gy IR (Figures 1 and 2). This indicates that the *Atm* deficiency sensitizes MSCs to differentiate in the niche, resulting in premature hair graying.

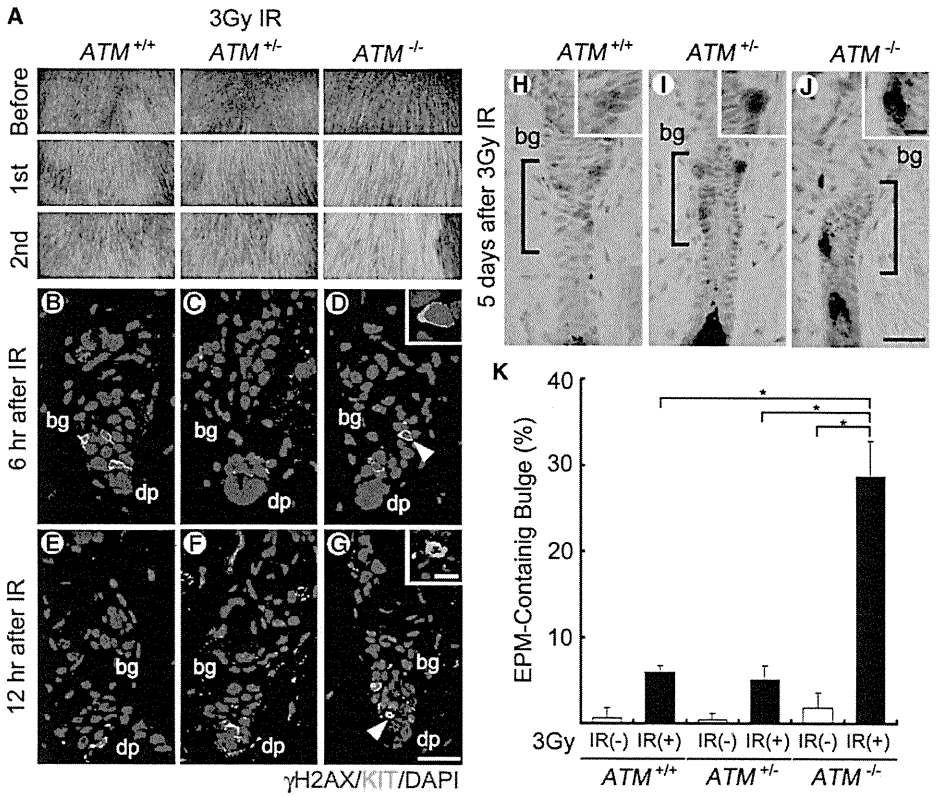

Figure 6. *Atm* Deficiency Sensitizes MSCs to IR-Induced Ectopic Differentiation in the Niche

(A) Changes of coat color in the 1st hair cycle (middle) and the 2nd hair cycle (bottom) after 3 Gy IR compared with before IR (top). Only $Atm^{-/-}$ mice show significant hair graying by 3 Gy IR, a dose normally insufficient to induce hair graying.

(B–G) Immunofluorescent staining of hair follicles for the detection of γH2AX damage foci formation in the bulge area after 3 Gy IR. Foci formation was retained abundantly in $Atm^{-/-}$ follicles including Kit^+ cells even at 12 hr (G). Insets show magnified views of γH2AX foci containing cells indicated with the white arrowheads.

(H–J) Dct-$lacZ^+$ cells in hair follicle bulges from $Atm^{+/+}$ (H), $Atm^{+/-}$ (I), and $Atm^{-/-}$ (J) mice at 5 days after 3 Gy IR. Dendritic EPMs were found in the bulge areas of $Atm^{-/-}$ hair follicles even with 3 Gy IR (J). Insets show magnified views of $lacZ^+$ cells in the bulge areas. The brackets indicate the bulge (bg).

(K) The frequency of hair follicles with EPM in the bulge area per total hair follicles after 3 Gy IR.

Error bars represent SEM; *$p < 0.001$ as calculated by Student's t test. Abbreviations: bg, bulge; dp, dermal papilla. Scale bars represent 25 μm in (G) and (J),5 μm in the inset of (G), and 10 μm in the inset of (J).

It is notable that DNA-damage foci formation was significantly induced in wild-type mouse skin with 3 Gy IR, a dose which does not induce any detectable changes in coat color and MSC number (Figures 6A and 6H), indicating that ATM efficiently protects MSCs from differentiation at low doses of IR. Furthermore, DNA-damage foci formation in the bulge area after 3 Gy IR was retained significantly longer in *Atm*-deficient mice (Figure 6G), as reported previously for cultured cells (Kuhne et al., 2004; Morrison et al., 2000). This suggests that the DNA-damage repair is inefficient in *Atm*-deficient mice as well as in vitro and that irreparable DNA-damage-induced signals may trigger the differentiation of damaged stem cells at the time of stem cell renewal to maintain the quality of the stem cell pool. Taken together, our data demonstrate that the DDR is involved in the determination of the fate of MSCs, suggesting the existence of a "stemness checkpoint" to maintain the stem cell quality and to prevent hair graying.

DISCUSSION

In Vivo Analysis of the Fate of MSCs under Genotoxic Stress

Stem cells can be characterized by their capacity to self-renew while generating many daughter cells that are committed to differentiation (Fuchs et al., 2004). Stem cell depletion due to the accumulation of DNA damage in the stem cell pool has been implicated in the degradation of tissue renewal capacity and in the appearance of aging-related phenotypes (Nijnik et al., 2007; Rossi et al., 2007a; Ruzankina et al., 2007, 2008). Stem cell exhaustion due to DNA damage has been attributed to apoptosis or senescence of stressed stem cells without detailed stem cell fate-tracing, probably because of technical difficulties (Ruzankina et al., 2008; Simonatto et al., 2007). In this study, we succeeded in analyzing the fate of MSCs under genotoxic stress and found that most MSCs commit to differentiation after stem

cell division. In this system, MSCs and their niche can be visualized and their differentiation status can be assessed by their morphology and most reliably by their pigmentation. The fate of stem cell progeny in the niche can be chronologically analyzed, as the timing of stem cell division can be effectively synchronized by the hair plucking method. MSCs divide at anagen II and the fate of their progeny is determined along with hair-cycle progression by their morphology and pigmentation in addition to lineage markers (Nishimura et al., 2002) (Figures 2 and S1). Furthermore, the functional level of the stem cell system can be assessed by the visible pigmentation of newly grown hair without sacrificing the animals. These advantages allowed us to chronologically analyze the fate of MSCs in hair follicles after exposure to genotoxic stress.

Genotoxic Stress Triggers a Melanocyte Differentiation Program in MSCs

We previously reported that EPMs appear in the stem cell niche prior to aging-related MSC depletion and resultant hair graying (Nishimura et al., 2005). In this study, we found that exposure to multiple genotoxins abrogates renewal of MSCs and induces the commitment of MSC progeny to differentiation in the niche accompanying hair-cycle progression. Our chronological analysis of MSCs revealed that IR induces the prolonged expression of melanogenic genes downstream of MITF and melanosome maturation in MSCs, indicating that MSCs mature into EPMs in the niche in response to IR. Furthermore, our studies with *Mc1r* mutant mice showed that IR-induced melanogenesis in MSC progeny in the niche depends on the *Mc1r*-mediated melanogenesis pathway, which is commonly used for melanocyte maturation and eumelanin pigment synthesis.

While epidermal melanocytes did not respond to IR compared to MSCs in the niche, our in vitro studies showed that IR induced an increased number of differentiated melanocytes in primary culture. Eller et al. also reported that UV and other DNA-damaging reagents can enhance melanogenesis in vitro (Eller et al., 1996). These findings suggest the existence of a cell-autonomous melanogenesis machinery in MSCs as well as the involvement of surrounding niche keratinocytes in the induction of EPMs. Though p53-dependent induction of POMC or KITL/SCF in keratinocytes for paracrine activation of melanocytes has been shown to mediate UV-induced skin tanning or some dark skin phenotypes in mice, respectively (Cui et al., 2007; McGowan et al., 2008), our data showed that the p53 pathway is transiently activated in MSCs after DNA damage but is not required for the induction of EPMs in the niche. Therefore, we conclude that the nodal point for damaged stem cell fate determination is located upstream of *Mc1r*-mediated melanogenic processes and is independent of the p53 pathway or melanocytic maturation level.

Stem Cell Differentiation with Defective Self-Renewal Is a Dominant Fate of Damaged MSCs

Genotoxic stress has been known to trigger cell-cycle arrest to allow DNA repair or induction of apoptosis or senescence in vitro (Campisi, 2003a; van Heemst et al., 2007). Similarly, stem cell senescence or apoptosis have been speculated to be major steps for stem cell depletion due to DNA damage in vivo (Ruzankina et al., 2008). Indeed, this theory is supported by an IR-induced "senescence"-like state characterized by SA-β-gal and p16 expression in purified cells expressing hematopoietic stem cell markers (Meng et al., 2003; Wang et al., 2006). Cell-cycle arrest of muscle progenitor cells under genotoxic stress also has been reported (Puri et al., 2002). However, it is not clear whether it represents a transient cellular response or the eventual fate of the cells and whether the cellular state explains the IR-induced tissue phenotypes.

In the MSC system, we found that stem cell differentiation is the major fate of MSCs under excessive genotoxic stress sufficient for the induction of hair graying. EPMs were induced in the niche within 1 week after IR without showing any significant induction of apoptosis markers or senescence markers. The EPMs are not associated with any morphological characteristics of cultured melanocytes arrested due to replicative senescence, including large, flat, and vacuolated morphology (Bennett and Medrano, 2002; Ha et al., 2008; Medrano et al., 1994). On the other hand, human melanocytic nevi express SA-β-gal and are considered to represent cellular senescence in vivo (Gray-Schopfer et al., 2006; Michaloglou et al., 2005), indicating that EPMs can be distinguished from senescent melanocytes. Though transient induction of p53 expression was found in MSCs after IR, EPMs were found even in *Trp53*-deficient mice and in *Ink4aArf*-deficient mice. Therefore, p53, $p16^{INK4a}$, or $p19^{ARF}$ are not required for the commitment of MSCs to differentiate in the niche in response to DNA damage. Instead, the existence of a stemness checkpoint was demonstrated in this study in mice with inefficient DDR. This new concept is supported by recent in vitro studies with embryonic stem cells, which lose their multipotency and differentiate after DNA damage in vitro (Lin et al., 2005). Therefore, the stemness checkpoint can be rather broadly responsible for DNA-damage-induced stem cell depletion for quality control of the stem cell pool in multiple somatic stem cell systems.

Checkpoint for Renewal of MSCs

Eukaryotic cells respond to DNA damage with a rapid activation of signaling cascades that initiate from the ATR and ATM protein kinases. *ATM* and *ATR* deficiency have been shown to degrade tissue renewal capacity through stem cell depletion with or without exogenous genotoxic stress (Ito et al., 2004; Ruzankina et al., 2007; Takubo et al., 2008). We found that *Atm*-deficient MSCs are sensitized to trigger differentiation in response to DNA damage. As DDR is affected by *Atm* deficiency (Kuhne et al., 2004; McKinnon, 2004; Morrison et al., 2000; Takubo et al., 2008), our data indicate that ATM efficiently protects MSCs from their differentiation in the niche by activating the downstream DDR pathways. Thus, the ATM-mediated DDR is a key for the determination of the fate of MSCs to prevent their premature differentiation and hair graying. Premature hair graying has been reported in *ATR* deficiency in the skin (Ruzankina et al., 2007) and in other repair-deficient progeria model mice, such as $XPD^{R722W/R722W}$ TTD mice (de Boer et al., 2002). As we have detected the significant appearance of EPMs in the bulge area of TTD mice (Figures 1Y and 1Z), stem cell differentiation might be a common general cellular mechanism for stem cell quality control. Therefore, the DNA-damage detection/repair machineries that serve as "caretakers" of the mammalian genome may

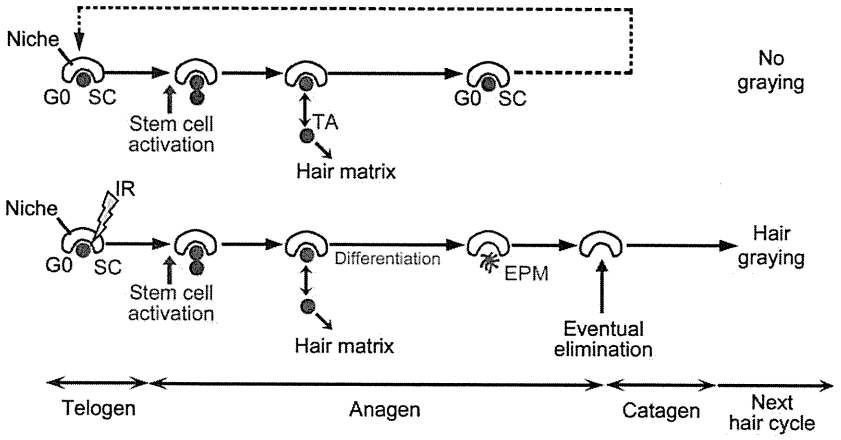

Figure 7. Stem Cell Differentiation Model under Genotoxic Stress

MSCs are maintained in an immature state in the niche throughout hair cycling in nonaged physiological conditions. Transient stem cell activation signals from the niche trigger self-renewal of stem cells at early anagen. The stem cell progeny that remain in the niche re-enter the quiescent state to maintain their stem cell integrity (upper panel). Under irreparable genotoxic stress, such as by IR or chronological aging, MSCs differentiate into EPMs ectopically in the niche without renewing themselves. These EPMs are subsequently eliminated at late anagen. Impaired self-renewal of MSCs through these processes results in hair graying in subsequent hair cycles (lower panel). Abbreviations: SC, stem cells; TA, transit-amplifying cells.

be functioning as a stemness checkpoint in some somatic stem cell systems.

Genotoxic Stress-Induced MSC Differentiation Underlies an Aging-Related Phenotype, Hair Graying

In addition to the aging-associated stem cell depletion typically seen in the MSC system (Nishimura et al., 2005), qualitative and quantitative changes of somatic stem cells have been reported in some stem cell systems, including HSCs, cardiac muscle, and skeletal muscle (Conboy et al., 2003; Morrison et al., 1996; Rossi et al., 2007b; Sussman and Anversa, 2004). Stresses on stem cell pools in genome maintenance failures have also been implicated in the decline of tissue renewal capacity and the accelerated appearance of aging-related phenotypes (Ruzankina et al., 2008). In this study, we discovered that hair graying, the most obvious aging phenotype, can be caused by the genomic damage response through stem cell differentiation, which suggests that physiological hair graying can be triggered by the accumulation of unavoidable DNA damage and DDR associated with aging through MSC differentiation. The EPM found in whisker follicles in aged wild-type mice (Figure 1X) is likely to represent the population. Therefore, our findings support the "stem cell aging hypothesis," which proposes that DNA damage in the long-lived stem cell population can be a major cause for the aging phenotype.

Then, what is the physiological role of stem cell differentiation in response to excessive/irreparable DNA damage? As shown schematically in Figure 7, genotoxic stress-induced EPMs were all eliminated from the niche at late anagen. Removing the damaged/stressed stem cells from the stem cell pool by triggering their differentiation (as the first step) and the eventual elimination of the differentiated damaged cells from the niche (as the second step) may be essential for the quality control of stem cell systems. The stemness checkpoint might be a key protection mechanism of stem cells against cancer development as well as a tissue-aging mechanism.

EXPERIMENTAL PROCEDURES

Animals

Dct-lacZ transgenic mice (a gift from Ian Jackson, MRC) have been described previously (Mackenzie et al., 1997). *XPD* mutant mice (a gift from Jan Hoeijmakers, EMC) (de Boer et al., 2002), *p53*-deficient mice (purchased from Taconic through IBL Japan) (Donehower et al., 1992), *INK4a/ARF*-deficient mice (obtained from the NCI Mouse Models of Human Cancers Consortium [MMHCC]) (Serrano et al., 1996), $MC1R^{e/e}$ mice (obtained from the Jackson Laboratory) (Robbins et al., 1993), and *Atm*-deficient mice (a gift from Peter J. McKinnon, St. Jude Children's Research Hospital) (Herzog et al., 1998) were crossed with *Dct-lacZ* transgenic mice, as described previously (Nishimura et al., 2005). Additional details are provided in the Supplemental Data.

Whole-Body X-Ray Irradiation of Mice

Whole-body X-ray irradiation (IR) was performed using a Hitachi MBR-1520 (Hitachi Medical) operating at 50 kVp, 20 mA with a 2.0 mm Al filter and a dose rate of 0.4 Gy/min. Mice were irradiated at 7–8 weeks old only after confirmation that the skin had a light pink color that indicates that hair follicles are synchronized at the telogen phase. One day after plucking the hair on the dorsal skin, the mice were irradiated (Argyris and Chase, 1960). Irradiation was carried out by placing each mouse in a thin-walled plastic box, after which the animals received whole-body X-rays at dose levels of 1 to 7 Gy. For analysis of the fate of MSCs in the 2nd or 3rd hair cycles, telogen hair depilation was performed with a 30 day interval following the first depilation and the skin was taken 5 days after the last telogen depilation.

Administration of DNA-Damaging Agents

After depilation was performed on the dorsal skin of 7-week-old mice, the mice were subjected to subcutaneous injection of 40 mg/kg body weight Busulfan (Wako Pure Chemicals), 4 mg/kg body weight Mitomycin C (Sigma-Aldrich), or 10 ml/kg body weight 1% hydrogen peroxide (Wako Pure Chemicals).

Immunohistochemical Analysis

Paraffin, frozen sections, and whole-mount β-galactosidase staining were performed as previously described (Nishimura et al., 2002, 2005). Additional details on the methods and antibodies used are provided in the Supplemental Data.

TUNEL Assay

For TUNEL staining (TdT-mediated dUTP-digoxigenin nick end labeling technique), we used the "*in situ* cell death detection kit, Fluorescein" (Roche Diagnostics). Signals were further amplified by Alexa Fluor 488-conjugated anti-fluorescein antibodies (Invitrogen).

Senescence-Associated β-Galactosidase Staining Assay

SA-β-Gal staining was performed on 10 μm-thick cryosections using the "Senescence Cells Histochemical Staining Kit" (Sigma-Aldrich), following the manufacturer's instructions.

Electron Microscopy

Twenty micrometer-thick frozen sections were prepared and stained in X-gal solution at 37°C for 12 hr. For electron microscopy, the sections were post-fixed

in 1% osmium tetroxide for 30 min, stained with 1% uranyl acetate for 20 min, dehydrated in a graded ethanol series, and finally embedded in epoxy resin. Semi-thin sections were stained with toluidine blue and observed by light microscopy. Ultra-thin sections were observed using a transmission electron microscope (JEOL) at 80 kV.

SUPPLEMENTAL DATA

Supplemental Data include Supplemental Experimental Procedures and nine figures and can be found with this article online at http://www.cell.com/supplemental/S0092-8674(09)00374-2.

ACKNOWLEDGMENTS

We thank Dr. Ian Jackson for the *Dct-lacZ* transgenic mice; Dr. Peter McKinnon and Dr. Atsushi Hirao for the *ATM*-deficient mice; Dr. Jan Hoeijmaker for the TTD mice; Dr. Vincent Hearing for antibodies; Dr. Naoko Ohtani, Dr. Kimi Yamakoshi, Dr. Keiyo Takubo, and Dr. Toshio Suda for immunostaining information; Ms. Lica Ishida, Ms. Misa Suzuki, Ms. Yuika Osaki, and Ms. Noriko Ikeda for technical assistance; Mr. Hideki Nakamura for mouse importation; and Dr. Richard Wong and Dr. Hiroyuki Nishimura for critical reading of the manuscript. The research was funded by grants from the Japanese Ministry of Education, Culture, Sports, Science and Technology (17689033, 19390293, 20012017), Uehara Memorial Foundation, and Kato Memorial Bioscience Foundation to E.K.N.

Received: September 9, 2008
Revised: December 15, 2008
Accepted: March 18, 2009
Published: June 11, 2009

REFERENCES

Argyris, T.S., and Chase, H.B. (1960). Effect of x-irradiation on differentating hair follicles. Anat. Rec. *136*, 445–451.

Barlow, C., Eckhaus, M.A., Schaffer, A.A., and Wynshaw Boris, A. (1999). Atm haploinsufficiency results in increased sensitivity to sublethal doses of ionizing radiation in mice. Nat. Genet. *21*, 359–360.

Bennett, D.C., and Medrano, E.E. (2002). Molecular regulation of melanocyte senescence. Pigment Cell Res. *15*, 242–250.

Boder, E., and Sedgwick, R.P. (1970). Ataxia-telangiectasia. (Clinical and immunological aspects). Psychiatr. Neurol. Med. Psychol. Beih. *13–14*, 8–16.

Campisi, J. (2003a). Cancer and ageing: rival demons? Nat. Rev. Cancer *3*, 339–349.

Campisi, J. (2003b). Cellular senescence and apoptosis: how cellular responses might influence aging phenotypes. Exp. Gerontol. *38*, 5–11.

Conboy, I.M., Conboy, M.J., Smythe, G.M., and Rando, T.A. (2003). Notch-mediated restoration of regenerative potential to aged muscle. Science *302*, 1575–1577.

Coolidge, W.D. (1925). High voltage cathode rays outside the generating tube. Science *62*, 441–442.

Cui, R., Widlund, H.R., Feige, E., Lin, J.Y., Wilensky, D.L., Igras, V.E., D'Orazio, J., Fung, C.Y., Schanbacher, C.F., Granter, S.R., et al. (2007). Central role of p53 in the suntan response and pathologic hyperpigmentation. Cell *128*, 853–864.

D'Orazio, J.A., Nobuhisa, T., Cui, R., Arya, M., Spry, M., Wakamatsu, K., Igras, V., Kunisada, T., Granter, S.R., Nishimura, E.K., et al. (2006). Topical drug rescue strategy and skin protection based on the role of Mc1r in UV-induced tanning. Nature *443*, 340–344.

de Boer, J., Andressoo, J.O., de Wit, J., Huijmans, J., Beems, R.B., van Steeg, H., Weeda, G., van der Horst, G.T., van Leeuwen, W., Themmen, A.P., et al. (2002). Premature aging in mice deficient in DNA repair and transcription. Science *296*, 1276–1279.

Donehower, L.A., Harvey, M., Slagle, B.L., McArthur, M.J., Montgomery, C.A., Jr., Butel, J.S., and Bradley, A. (1992). Mice deficient for p53 are developmentally normal but susceptible to spontaneous tumours. Nature *356*, 215–221.

Eller, M.S., Ostrom, K., and Gilchrest, B.A. (1996). DNA damage enhances melanogenesis. Proc. Natl. Acad. Sci. USA *93*, 1087–1092.

Fuchs, E., Tumbar, T., and Guasch, G. (2004). Socializing with the neighbors: stem cells and their niche. Cell *116*, 769–778.

Gray-Schopfer, V.C., Cheong, S.C., Chong, H., Chow, J., Moss, T., Abdel-Malek, Z.A., Marais, R., Wynford-Thomas, D., and Bennett, D.C. (2006). Cellular senescence in naevi and immortalisation in melanoma: a role for p16? Br. J. Cancer *95*, 496–505.

Ha, L., Merlino, G., and Sviderskaya, E.V. (2008). Melanomagenesis: overcoming the barrier of melanocyte senescence. Cell Cycle *7*, 1944–1948.

Hasty, P., Campisi, J., Hoeijmakers, J., van Steeg, H., and Vijg, J. (2003). Aging and genome maintenance: lessons from the mouse? Science *299*, 1355–1359.

Hearing, V.J. (2005). Biogenesis of pigment granules: a sensitive way to regulate melanocyte function. J. Dermatol. Sci. *37*, 3–14.

Herzog, K.H., Chong, M.J., Kapsetaki, M., Morgan, J.I., and McKinnon, P.J. (1998). Requirement for Atm in ionizing radiation-induced cell death in the developing central nervous system. Science *280*, 1089–1091.

Hirobe, T., Abe, H., Wakamatsu, K., Ito, S., Kawa, Y., Soma, Y., and Mizoguchi, M. (2007). Excess tyrosine rescues the reduced activity of proliferation and differentiation of cultured recessive yellow melanocytes derived from neonatal mouse epidermis. Eur. J. Cell Biol. *86*, 315–330.

Itahana, K., Campisi, J., and Dimri, G.P. (2004). Mechanisms of cellular senescence in human and mouse cells. Biogerontology *5*, 1–10.

Ito, K., Hirao, A., Arai, F., Matsuoka, S., Takubo, K., Hamaguchi, I., Nomiyama, K., Hosokawa, K., Sakurada, K., Nakagata, N., et al. (2004). Regulation of oxidative stress by ATM is required for self-renewal of haematopoietic stem cells. Nature *431*, 997–1002.

Kinzler, K.W., and Vogelstein, B. (1998). Landscaping the cancer terrain. Science *280*, 1036–1037.

Kuhne, M., Riballo, E., Rief, N., Rothkamm, K., Jeggo, P.A., and Lobrich, M. (2004). A double-strand break repair defect in ATM-deficient cells contributes to radiosensitivity. Cancer Res. *64*, 500–508.

Levy, C., Khaled, M., and Fisher, D.E. (2006). MITF: master regulator of melanocyte development and melanoma oncogene. Trends Mol. Med. *12*, 406–414.

Lin, T., Chao, C., Saito, S., Mazur, S.J., Murphy, M.E., Appella, E., and Xu, Y. (2005). p53 induces differentiation of mouse embryonic stem cells by suppressing Nanog expression. Nat. Cell Biol. *7*, 165–171.

Lowe, S.W., Cepero, E., and Evan, G. (2004). Intrinsic tumour suppression. Nature *432*, 307–315.

Mackenzie, M.A., Jordan, S.A., Budd, P.S., and Jackson, I.J. (1997). Activation of the receptor tyrosine kinase Kit is required for the proliferation of melanoblasts in the mouse embryo. Dev. Biol. *192*, 99–107.

Maier, B., Gluba, W., Bernier, B., Turner, T., Mohammad, K., Guise, T., Sutherland, A., Thorner, M., and Scrable, H. (2004). Modulation of mammalian life span by the short isoform of p53. Genes Dev. *18*, 306–319.

Martin, G.M. (2005). Genetic modulation of senescent phenotypes in *Homo sapiens*. Cell *120*, 523–532.

McGowan, K.A., Li, J.Z., Park, C.Y., Beaudry, V., Tabor, H.K., Sabnis, A.J., Zhang, W., Fuchs, H., de Angelis, M.H., Myers, R.M., et al. (2008). Ribosomal mutations cause p53-mediated dark skin and pleiotropic effects. Nat. Genet. *40*, 963–970.

McKinnon, P.J. (2004). ATM and ataxia telangiectasia. EMBO Rep. *5*, 772–776.

Medrano, E.E., Yang, F., Boissy, R., Farooqui, J., Shah, V., Matsumoto, K., Nordlund, J.J., and Park, H.Y. (1994). Terminal differentiation and senescence in the human melanocyte: repression of tyrosine-phosphorylation of the extracellular signal-regulated kinase 2 selectively defines the two phenotypes. Mol. Biol. Cell *5*, 497–509.

Meng, A., Wang, Y., Van Zant, G., and Zhou, D. (2003). Ionizing radiation and busulfan induce premature senescence in murine bone marrow hematopoietic cells. Cancer Res. *63*, 5414–5419.

Michaloglou, C., Vredeveld, L.C., Soengas, M.S., Denoyelle, C., Kuilman, T., van der Horst, C.M., Majoor, D.M., Shay, J.W., Mooi, W.J., and Peeper, D.S. (2005). BRAFE600-associated senescence-like cell cycle arrest of human naevi. Nature *436*, 720–724.

Morrison, C., Sonoda, E., Takao, N., Shinohara, A., Yamamoto, K., and Takeda, S. (2000). The controlling role of ATM in homologous recombinational repair of DNA damage. EMBO J. *19*, 463–471.

Morrison, S.J., Wandycz, A.M., Akashi, K., Globerson, A., and Weissman, I.L. (1996). The aging of hematopoietic stem cells. Nat. Med. *2*, 1011–1016.

Nijnik, A., Woodbine, L., Marchetti, C., Dawson, S., Lambe, T., Liu, C., Rodrigues, N.P., Crockford, T.L., Cabuy, E., Vindigni, A., et al. (2007). DNA repair is limiting for haematopoietic stem cells during ageing. Nature *447*, 686–690.

Nishimura, E.K., Jordan, S.A., Oshima, H., Yoshida, H., Osawa, M., Moriyama, M., Jackson, I.J., Barrandon, Y., Miyachi, Y., and Nishikawa, S. (2002). Dominant role of the niche in melanocyte stem-cell fate determination. Nature *416*, 854–860.

Nishimura, E.K., Granter, S.R., and Fisher, D.E. (2005). Mechanisms of hair graying: incomplete melanocyte stem cell maintenance in the niche. Science *307*, 720–724.

Potten, C.S. (1970). Radiation depigmentation of mouse hair: effect of the hair growth cycle on the sensitivity. J. Invest. Dermatol. *55*, 410–418.

Puri, P.L., Bhakta, K., Wood, L.D., Costanzo, A., Zhu, J., and Wang, J.Y. (2002). A myogenic differentiation checkpoint activated by genotoxic stress. Nat. Genet. *32*, 585–593.

Robbins, L.S., Nadeau, J.H., Johnson, K.R., Kelly, M.A., Roselli-Rehfuss, L., Baack, E., Mountjoy, K.G., and Cone, R.D. (1993). Pigmentation phenotypes of variant extension locus alleles result from point mutations that alter MSH receptor function. Cell *72*, 827–834.

Rossi, D.J., Bryder, D., Seita, J., Nussenzweig, A., Hoeijmakers, J., and Weissman, I.L. (2007a). Deficiencies in DNA damage repair limit the function of haematopoietic stem cells with age. Nature *447*, 725–729.

Rossi, D.J., Bryder, D., and Weissman, I.L. (2007b). Hematopoietic stem cell aging: mechanism and consequence. Exp. Gerontol. *42*, 385–390.

Ruzankina, Y., Pinzon-Guzman, C., Asare, A., Ong, T., Pontano, L., Cotsarelis, G., Zediak, V.P., Velez, M., Bhandoola, A., and Brown, E.J. (2007). Deletion of the developmentally essential gene ATR in adult mice leads to age-related phenotypes and stem cell loss. Cell Stem Cell *1*, 113–126.

Ruzankina, Y., Asare, A., and Brown, E.J. (2008). Replicative stress, stem cells and aging. Mech. Ageing Dev. *129*, 460–466.

Schumacher, B., Garinis, G.A., and Hoeijmakers, J.H. (2008). Age to survive: DNA damage and aging. Trends Genet. *24*, 77–85.

Serrano, M., Lee, H., Chin, L., Cordon-Cardo, C., Beach, D., and DePinho, R.A. (1996). Role of the INK4a locus in tumor suppression and cell mortality. Cell *85*, 27–37.

Sharpless, N.E., and DePinho, R.A. (2007). How stem cells age and why this makes us grow old. Nat. Rev. Mol. Cell Biol. *8*, 703–713.

Simonatto, M., Latella, L., and Puri, P.L. (2007). DNA damage and cellular differentiation: more questions than responses. J. Cell. Physiol. *213*, 642–648.

Sussman, M.A., and Anversa, P. (2004). Myocardial aging and senescence: where have the stem cells gone? Annu. Rev. Physiol. *66*, 29–48.

Takubo, K., Ohmura, M., Azuma, M., Nagamatsu, G., Yamada, W., Arai, F., Hirao, A., and Suda, T. (2008). Stem cell defects in ATM-deficient undifferentiated spermatogonia through DNA damage-induced cell-cycle arrest. Cell Stem Cell *2*, 170–182.

Taylor, A.M., Harnden, D.G., Arlett, C.F., Harcourt, S.A., Lehmann, A.R., Stevens, S., and Bridges, B.A. (1975). Ataxia telangiectasia: a human mutation with abnormal radiation sensitivity. Nature *258*, 427–429.

van Heemst, D., den Reijer, P.M., and Westendorp, R.G. (2007). Ageing or cancer: a review on the role of caretakers and gatekeepers. Eur. J. Cancer *43*, 2144–2152.

Vance, K.W., and Goding, C.R. (2004). The transcription network regulating melanocyte development and melanoma. Pigment Cell Res. *17*, 318–325.

Wang, Y., Schulte, B.A., LaRue, A.C., Ogawa, M., and Zhou, D. (2006). Total body irradiation selectively induces murine hematopoietic stem cell senescence. Blood *107*, 358–366.

Ward, J.F. (1988). DNA damage produced by ionizing radiation in mammalian cells: identities, mechanisms of formation, and reparability. Prog. Nucleic Acid Res. Mol. Biol. *35*, 95–125.

Yamaguchi, Y., Brenner, M., and Hearing, V.J. (2007). The regulation of skin pigmentation. J. Biol. Chem. *282*, 27557–27561.

Correspondence

Scleroedema adultorum associated with sarcoidosis

doi: 10.1111/j.1365-2230.2009.03423.x

Sarcoidosis is a systemic granulomatous disease of unknown aetiology that displays a wide variety of skin features including maculopapules, nodules, plaques, subcutaneous nodules, infiltrative scars, and lupus pernio.[1] We report a case of sarcoidosis with subcutaneous induration of the neck.

A 62-year-old Japanese man presented with a 6-month history of asymptomatic, firm indurations on the neck. He had first noticed these skin lesions after bilateral symmetrical hilar lymph-node enlargement was found during routine chest radiography. Transbronchial biopsies resulted in the histological identification of non-caseating granulomas compatible with sarcoidosis. The patient had no history of diabetes mellitus or preceding infection.

On physical examination, symmetrical, hard, nonpitting indurations of the skin were found on the posterior neck (Fig. 1a). The patient's general health was good.

Results of routine laboratory studies including angiotensin-converting enzyme and tuberculin response gave normal results, and there was no evidence of monoclonal proteinaemia. Computed tomography scans showed bilateral hilar lymphadenopathy but there was no other lymphadenopathy noted.

Histological examination of skin-biopsy specimens taken from the posterior neck revealed swelling of the dermal collagen bundles without increase in fibroblast numbers, and the subcutaneous fat had been replaced by collagen fibres (Fig. 1b). A diagnosis of SA was made. Treatment was started with steroid ointment or 9 months, but without evident improvement.

SA is a rare disorder of unknown cause, but often complicates diabetes mellitus. In such cases, the lesions are usually limited to neck and upper back, and tend to be persistent.[2] In contrast, in SA not associated with diabetes mellitus, the lesions often spread to the face, trunk and upper arms, but may spontaneously subside.[3,4] However, in spite of no obvious association with diabetes mellitus, our patient had intractable induration distributed over a localized area. Interestingly, in this case, development of the skin lesion was coincidental with the diagnosis of sarcoidosis. The clinical appearance was indicative of scleroedema. There have been no previous reports of any association between SA and sarcoidosis. Therefore, we first suspected a subcutaneous form of sarcoidosis rather than scleroedema. However, the histopathological findings confirmed a diagnosis of scleroedema.

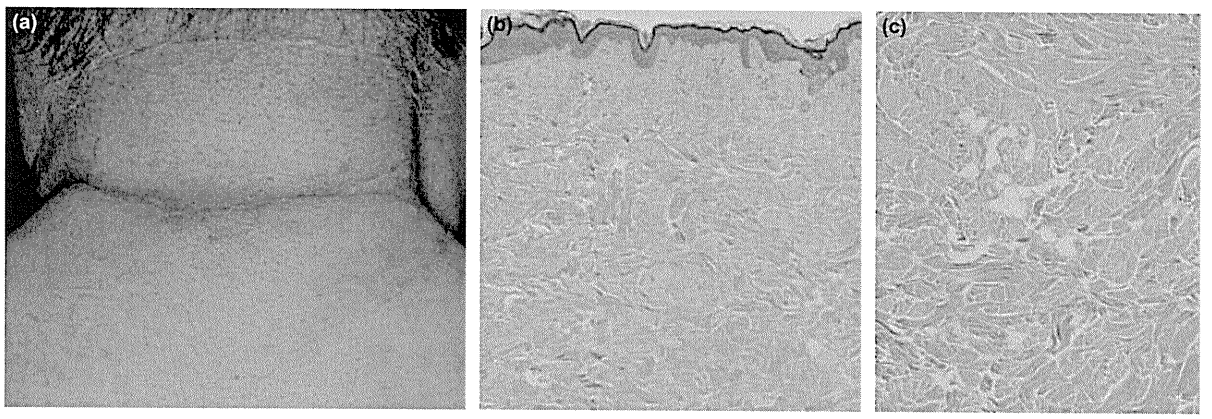

Figure 1 (a) Symmetrical, hard, nonpitting induration on the posterior side of the neck; (b) inflammatory cell infiltration in the upper dermis and swelling of collagen bundles in the lower dermis; (c) swelling of the dermal collagen bundles without any increase in fibroblast numbers, and the replacing of subcutaneous fatty tissues by collagen fibres.

Sarcoidosis is known to be complicated by a variety of immunological diseases including malignant lymphoma, autoimmune diseases and multiple myeloma, and scleroedema is associated with infections, paraproteinaemia and multiple myeloma. Some previous studies have shown an increase in amounts of proα1(I) collagen mRNA in both sarcoidosis and scleroedema lesions.[5] Some common factors in the pathogenesis of two diseases might therefore be involved in this patient.

D. Inokuma, D. Sawamura,* A. Shibaki, R. Abe and H. Shimizu

*Department of Dermatology, Hokkaido University Graduate School of Medicine, North 15 West 7, Kita-ku, Sapporo, 060-8638, Japan; and *Department of Dermatology, Hirosaki University Graduate School of Medicine, Hirosaki CIty, Japan*

E-mail: inokuma@med hokudai.ac.jp

Conflict of interest: none declared.

Accepted for publication 7 January 2009

References

1 Young RJ III, Gilson RT, Yanase D *et al.* Cutaneous sarcoidosis. *Int J Dermatol* 2001; **40**: 249–53.

2 Farrell AM, Branfoot AC, Moss J *et al.* Scleredema diabeticorum of Buschke confined to the thighs. *Br J Dermatol* 1996; **134**: 1113–15.

3 Basarab T, Burrows NP, Munn SE *et al.* Systemic involvement in scleredema of Buschke associated with IgG-kappa paraproteinaemia. *Br J Dermatol* 1997; **136**: 939–42.

4 Ratip S, Akin H, Ozdemirli M *et al.* Scleredema of Buschke associated with Waldenstrom's macroglobulinaemia. *Br J Dermatol* 2000; **143**: 450–2.

5 Tasanen PO. Demonstration of increased levels of type I collagen mRNA using quantitative polymerase chain reaction in fibrotic and granulomatous skin diseases. *Br J Dermatol* 1998; **139**: 23–6.

Table 2 Confounding factors in skin sensitivity testing

Menstrual cycle[4]
Concentration of test substance[4,6,10]
Dose of test substance[6,10]
Batch volume[6]
Purity of test substance[6,10]
Test substance vehicle[6]
Length of exposure[6]
Time of occlusion[6]
Release of test substance from chamber[6]
Enhancement of penetration[6]
Method of evaluation[4–7]
Time of evaluation after exposure[2,4,6,7]
Humidity[6,10]
Water vapour gradient[6]
Impairment of skin barrier[6]
Anatomical site[6]
Intrinsic level of skin sensitivity[6]
Booster effect[8]
Individual variation[8,10]
Skin temperature[6]
Ultraviolet exposure[6]
Age[6]
Sex[6]
Race[6]
Circadian rhythms[10]
Concomitant medications[10]

effect of reproductive hormones on skin disorders have been somewhat hampered, however, by the fact that individual patient sensitivity varies widely and by a body of research that has employed diverse research parameters, such as dosage, testing sites, concentration, vehicle of irritant delivery, and method of assessment. Further research, with strict attention to standardizing experimental parameters and limiting compounding factors, will help to elucidate the biochemical basis for the observed effects of progesterone and oestrogen levels on skin health. Dermatologists should be aware that the menstrual cycle can affect the sensitivity of women to primary irritants and can affect their allergic response.

M.A. Farage
E. Berardesca*
H.I. Maibach†

Feminine Clinical Sciences,
The Procter and Gamble Company,
Winton Hill Business Centre,
6110 Centre Hill Road, PO Box 136,
Cincinnati, OH 45224, U.S.A.
**San Gallicano Dermatological Institute,*
Rome, Italy
†*Department of Dermatology,*
School of Medicine, University of California,
San Francisco, CA, U.S.A.
E-mail: farage.m@pg.com

References

1 Itsekson A, Lazarov A, Cordoba M *et al.* Premenstrual syndrome and associated skin diseases related to hypersensitivity to female sex hormones. *J Reprod Med* 2004; **49**:195–9.
2 Kirmaz C, Yuksel H, Mete N *et al.* Is the menstrual cycle affecting the skin prick test reactivity? *Asian Pac J Allergy Immunol* 2004; **22**:197–203.
3 Agarwal S, Shukla HS, Verma M *et al.* Investigation of lymphocyte subpopulations and hypersensitivity skin tests during the menstrual cycle and pregnancy. *Ann Chir Gynaecol* 1982; **71**:117–21.
4 Bonamonte D, Foti C, Antelmi AR *et al.* Nickel contact allergy and menstrual cycle. *Contact Dermatitis* 2005; **52**:309–13.
5 Kiriyama K, Sugiura H, Uehara M. Premenstrual deterioration of skin symptoms in female patients with atopic dermatitis. *Dermatology* 2003; **206**:110–12.
6 Agner T. Noninvasive measuring methods for the investigation of irritant patch test reactions. a study of patients with hand eczema, atopic dermatitis and controls. *Acta Derm Venereol (Stockh)* 1992; **173** (Suppl.):1–26.
7 Tamer E, Ikizoglu G, Toy GG *et al.* Comparison of nickel patch test reactivity in phases of the menstrual cycle. *Int J Dermatol* 2003; **42**:455–8.
8 Rohold AE, Halkier-Sørensen L, Andersen KE *et al.* Nickel patch test reactivity and the menstrual cycle. *Acta Derm Venereol (Stockh)* 1994; **74**:383–5.
9 Kemmett D, Tidman MJ. The influence of the menstrual cycle and pregnancy on atopic dermatitis. *Br J Dermatol* 1991; **125**:59–61.
10 Hindsén M, Bruze M, Christensen OB. Individual variation in nickel patch test reactivity. *Am J Contact Dermat* 1999; **10**:62–7.
11 Drexler B, Landthaler M, Hohenleutner S. The menstrual cycle and the skin. In: *The Vulva: Anatomy, Physiology, and Pathology* (Farage M, Maibach H, eds). New York: Informa Healthcare, 2006; 167–79.

Key words: *allergic response, atopic dermatitis, menstruation, oestrogen, progesterone, skin testing*

Conflicts of interest: none declared.

Autoantibodies against type XVII collagen C-terminal domain in a patient with bullous pemphigoid associated with psoriasis vulgaris

DOI: 10.1111/j.1365-2133.2008.08961.x

Sir, Bullous pemphigoid (BP) has been reported to develop occasionally in patients with psoriasis vulgaris.[1,2] BP with psoriasis vulgaris is typically associated with autoantibodies against type XVII collagen (Col17) with the main antigenic site occurring within the noncollagenous 16a (NC16a) domain.[2] We report the first patient with BP associated with psoriasis vulgaris whose autoantibodies targeted the C-terminal domain of Col17. In addition, our patient also exhibited gastric carcinoma, similar to other patients with BP in whom internal malignancies have been reported.

A 64-year-old Japanese man with 6-year history of psoriasis vulgaris presented with an extensive eruption that had started 3 days previously with numerous pruritic, tense bullae on a background of psoriatic plaques over his entire body (Fig. 1a). Palmoplantar bullous lesions were also severe (Fig. 1b) and there were erosions on his lips (Fig. 1c) but not on the genital area nor on the oral mucosa. He had never received psoralen + ultraviolet (UV) A (PUVA) or narrowband UVB therapy.

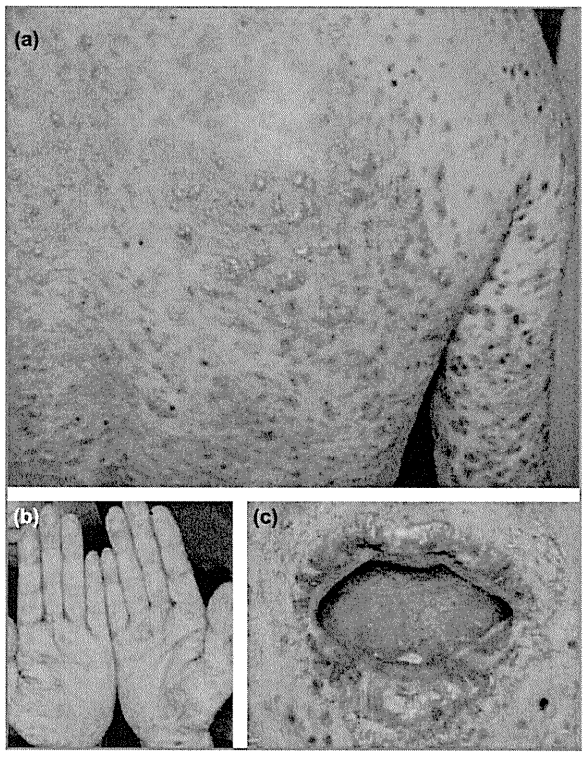

Fig 1. Clinical features. (a) Tense bullae and psoriatic plaques on the back. (b) Bullae and oedematous erythema on the palms. (c) Erosion on the lips.

Skin biopsies were taken from two psoriatic plaques, one with and one without a blister. Histopathology of the first biopsy showed subepidermal blistering with an abundant infiltrate mainly of neutrophils and lymphocytes, and a small number of eosinophils. Parakeratosis and regular acanthosis were also seen around the roof of the blister (Fig. 2a). Histology of the typical psoriatic plaque without a blister demonstrated psoriatic-like regular acanthosis, parakeratosis, a subepidermal neutrophilic abscess and limited eosinophilic infiltration in the dermis (Fig. 2b).

Direct immunofluorescence (IF) from the specimen around the blister revealed linear C3 and IgG deposits along the basement membrane zone but no IgA or IgM deposits (Fig. 3a). Indirect IF (IIF), using normal human skin as substrate, demonstrated a high titre of circulating IgG autoantibodies against the dermal–epidermal junction (> 1 : 160). IIF on 1 mol L^{-1} NaCl-split skin revealed linear IgG deposition on both epidermal and dermal sides of the split (> 1 : 40) (Fig. 3b). Using an enzyme-linked immunosorbent assay (ELISA) to measure IgG against the NC16a domain of Col17, the index value was low at 12 IU (normal < 9). Immunoblot assays revealed that the patient sera reacted with the recombinant C-terminal domain of Col17[3] and with BP230 using human epidermal extracts (Fig. 3c). Autoantibodies against the 290-kDa epidermolysis bullosa acquisita (EBA) antigen, anti-p200 pemphigoid antigen, laminin 332 chains and recombinant Col17 NC16a domain were not detected by immunoblot.

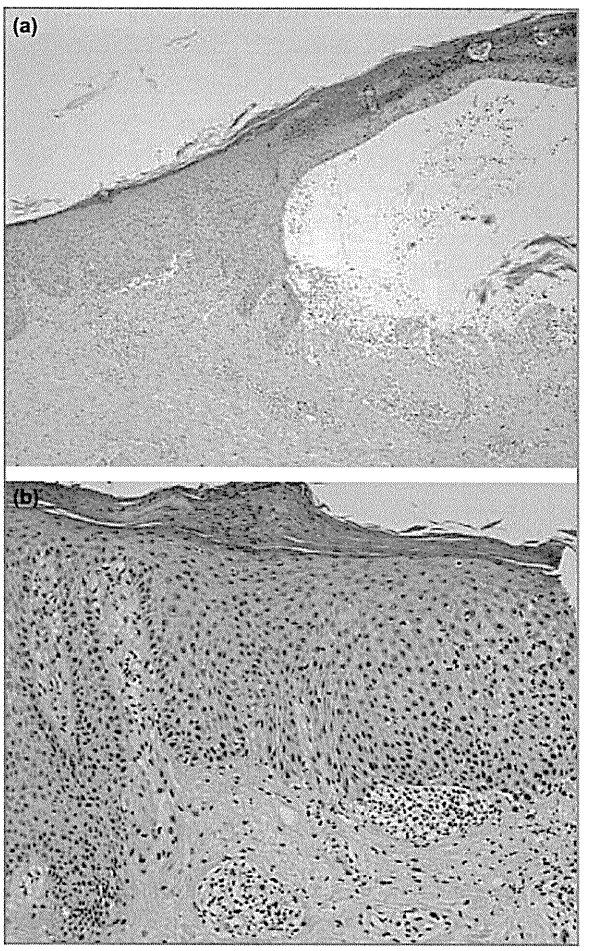

Fig 2. (a) Subepidermal blister with an abundant infiltrate of neutrophils and lymphocytes in a specimen from a bulla on the psoriatic plaque. (b) Subepidermal neutrophilic abscess with neutrophils in a specimen from a psoriatic plaque without bullae (haematoxylin and eosin).

The patient also had the complication of gastric cancer discovered through gastric fibrescope examination. Biopsy revealed a carcinoma *in situ*. Computed tomography did not show any metastases of this gastric cancer. We diagnosed our patient as having BP with antibodies positive for the anti-Col17 C-terminal domain, associated with psoriasis vulgaris and gastric carcinoma. Administration of oral prednisolone 35 mg daily (0·5 mg kg^{-1} daily) improved skin and oral involvement and he remained well controlled with prednisolone 10 mg daily. The gastric carcinoma *in situ* was removed endoscopically.

It is widely thought that BP is a subepidermal autoimmune blistering disease with autoantibodies against Col17 involving the skin and mucosa. BP is particularly associated with autoantibodies to Col17, with the major antigenic site being within the extracellular NC16a domain. ELISA using NC16a recombinant protein fragments is a valuable tool for the definite diagnosis of BP and for repeated, consistent monitoring of disease activity. Recent studies, however, have demonstrated

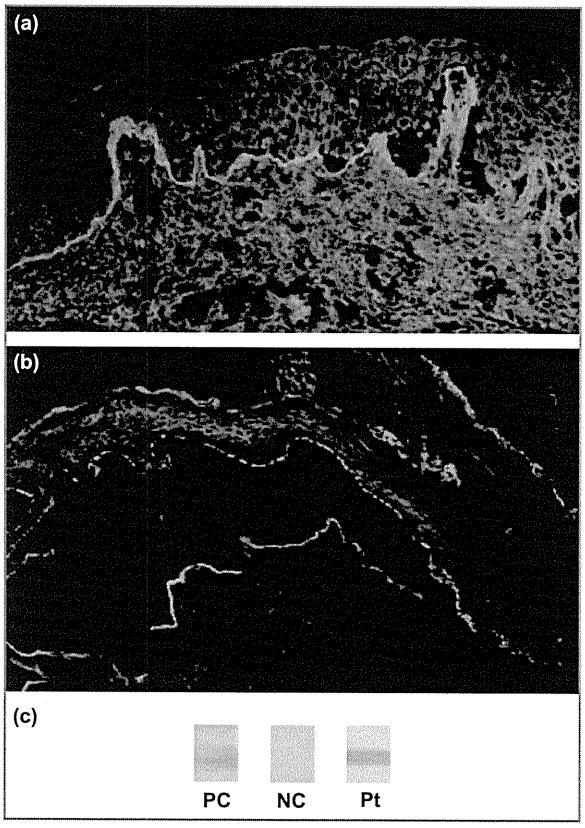

Fig 3. (a) Direct immunofluorescence from a specimen around the blister revealed a linear IgG deposition along the basement membrane zone. (b) Indirect immunofluorescence on 1 mol L^{-1} NaCl-split skin revealed a linear IgG deposition on both sides of the epidermal and the dermal separation. (c) Immunoblot analysis using Col17 C-terminal recombinant protein. Lane 1, serum from a patient with mucous membrane pemphigoid (PC); lane 2, normal control serum (NC); lane 3, the patient's serum (Pt).

that the reactivity of BP sera is not restricted to the NC16a domain.[4] It has been reported that 9% of BP sera do not react with the NC16a domain in immunoblot analysis. Moreover, in 20 cases of mucous membrane pemphigoid, nine sera recognized the NC16a domain, and three of the 20 sera reacted with epitopes in either the mid-portion or the C-terminus of Col17.[5]

IIF on 1 mol L^{-1} NaCl-split skin revealed linear deposition of antibodies to the C-terminal domain of Col17 on only the epidermal side but, in our case, IIF revealed deposition on both epidermal and dermal sides of the split. We performed immunoblot assays of autoantibodies against the 290-kDa EBA antigen, anti-p200 pemphigoid antigen, laminin 332 chains and recombinant Col17 NC16a domain, but all were negative. In a previous report, antibasement membrane zone antibodies reacting to both the dermal and epidermal sides were demonstrated by IIF in 2% of cases of BP, and the C-terminal domain of Col17 is present in the lamina densa under the lamina lucida, so it is possible for antibodies to the C-terminal to react to both epidermal and dermal sides in split-skin IIF.

The combination of psoriasis with autoimmune subepidermal bullous disease, for instance BP,[1,2] linear IgA bullous dermatosis[6,7] or EBA,[8] has been reported. Recently, especially in the Japanese population, several cases of the combination of psoriasis with anti-p200 pemphigoid have been reported.[1,2,9] Autoantibodies to p200 protein were not detected in the present case by immunoblot assay. To the best of our knowledge there have not been any previous reports of patients with BP associated with psoriasis vulgaris whose sera reacted with the C-terminal domain of Col17. There have been several reports on the association between BP and psoriasis vulgaris but the pathogenic significance of this relationship is unknown. There have been no reports which showed the association of other diseases with antibodies to the C-terminal domain, and the causal relationship is also not clear. PUVA or UVB therapy for psoriasis may trigger the development of BP but our patient had not received any PUVA or UVB therapy.[10]

We have described the first case of psoriasis vulgaris with BP autoantibodies against the C-terminal of Col17 protein which was successfully treated. We hope that any future cases may shed more light on the pathomechanisms of this disease.

Department of Dermatology,
Hokkaido University Graduate School of Medicine,
N 15 W 7, Kita-ku, Sapporo 060-8638, Japan
**Sapporo Railway Hospital, Sapporo, Japan*
†Department of Dermatology,
Kurume University School of Medicine, Kurume, Japan
E-mail: inokuma@med.hokudai.ac.jp

D. Inokuma
K. Kodama*
K. Natsuga
M. Kasai*
M. Abe*
W. Nishie
R. Abe
T. Hashimoto†
H. Shimizu

References

1 Kirtschig G, Chow ET, Venning VA *et al.* Acquired subepidermal bullous diseases associated with psoriasis: a clinical, immunopathological and immunogenetic study. *Br J Dermatol* 1996; **135**:738–45.
2 Yasuda H, Tomita Y, Shibaki A *et al.* Two cases of subepidermal blistering disease with anti-p200 or 180-kD bullous pemphigoid antigen associated with psoriasis. *Dermatology* 2004; **209**:149–55.
3 Nie Z, Hashimoto T. IgA antibodies of cicatricial pemphigoid sera specifically react with C-terminus of BP180. *J Invest Dermatol* 1999; **112**:254–5.
4 Calabresi V, Carrozzo M, Cozzani E *et al.* Oral pemphigoid autoantibodies preferentially target BP180 ectodomain. *Clin Immunol* 2007; **122**:207–13.
5 Shinojima Y, Ochiai T, Kawamura A *et al.* A case of bullous pemphigoid associated with autoantibodies targeting antigenic sites other than the NC16a domain of BP180. *Clin Exp Dermatol* 2005; **30**:503–5.
6 Cooke N, Jenkinson H, Wojnarowska F *et al.* Coexistence of psoriasis and linear IgA disease in a patient with recent herpes zoster infection. *Clin Exp Dermatol* 2005; **30**:643–5.
7 Takagi Y, Sawada S, Yamauchi M *et al.* Coexistence of psoriasis and linear IgA bullous dermatosis. *Br J Dermatol* 2000; **142**:513–16.
8 Hoshina D, Sawamura D, Nomura T *et al.* Epidermolysis bullosa acquisita associated with psoriasis vulgaris. *Clin Exp Dermatol* 2007; **32**:516–18.

9 Yamane N, Sawamura D, Nishie W *et al.* Anti-p200 pemphigoid in a 17-year-old girl successfully treated with systemic corticosteroid and dapsone. *Br J Dermatol* 2007; **156**:1075–8.
10 Perl S, Rappersberger K, Fodinger D *et al.* Bullous pemphigoid induced by PUVA therapy. *Dermatology* 1996; **193**:245–7.

Key words: *bullous pemphigoid, Col17 C-terminal domain, psoriasis vulgaris*

Conflicts of interest: none declared.

Folliculosebaceous cystic hamartoma differentiates toward the infundibulum, sebaceous duct and sebaceous cells: immunohistochemical study of keratins and filaggrin

DOI: 10.1111/j.1365-2133.2008.08964.x

SIR, Folliculosebaceous cystic hamartoma (FSCH) is a rare cutaneous hamartoma with varying proportions of epithelial components and mesenchymal overgrowth.[1] The epithelial components consist of an infundibular cystic structure to which mature sebaceous lobules are attached via sebaceous ducts. The histogenesis of FSCH remains unclear.

We report a case of FSCH occurring on the nasolabial fold in an elderly Japanese man. To determine the differentiation of FSCH, we performed an immunohistochemical study of keratins[2,3] and filaggrin[4] (filament aggregating protein). To our knowledge, this is the first report of FSCH with an immunohistochemical study of keratins and filaggrin. Since this tumour was first described by Kimura *et al.* in 1991,[1] about 30 cases have been reported.[5]

A 78-year-old man presented with a 3-year history of a slow-growing, pink-yellow, elastic hard, pedunculated asymptomatic nodule 17 × 13 mm in size on the right side of his nose. Specimens were fixed in neutral formalin, embedded in paraffin and stained with haematoxylin and eosin. Serial sections were used for the immunohistochemical study. We used 10 antikeratin antibodies: 34βB4 [keratin 1 (K1)], LP5K (K7), LP3K (K8), LHP1 (K10), LL022 (K14), LHK15 (K15), LL025

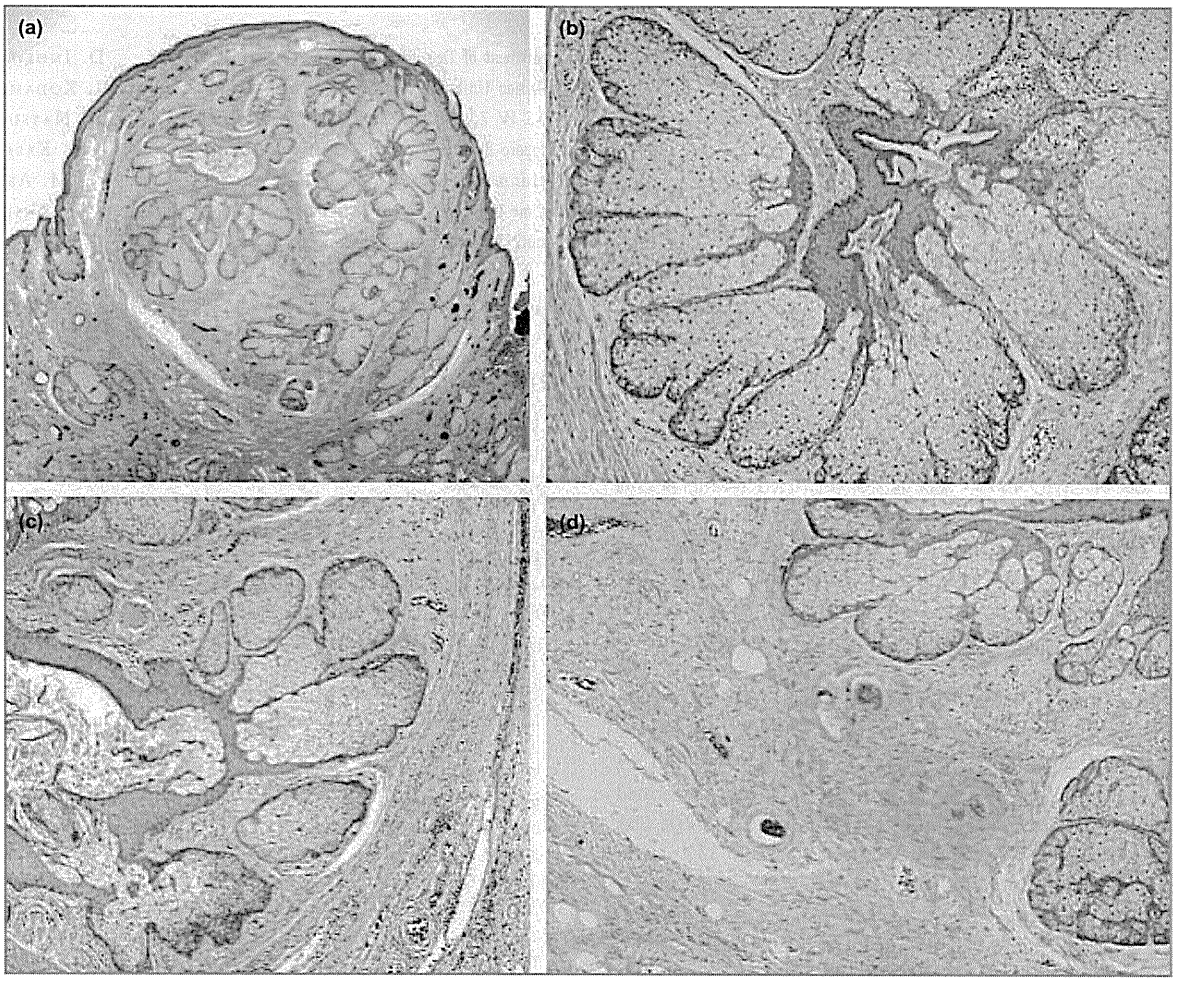

Fig 1. Haematoxylin and eosin staining. (a) The tumour in the dermis and was sharply demarcated from adjacent compressed fibrous tissue of the surrounding dermis by prominent clefts. (b) 'Folliculosebaceous units', which consist of infundibular cystic structures, sebaceous duct-like structures and hypertrophic sebaceous lobules, surrounded by lamellar fibroplasia. (c) Sebaceous duct-like structure. (d) Fibroepithelial unit.

Bowen's Disease of the Nail Matrix Presenting as Melanonychia: Detection of Human Papillomavirus Type 56

Daisuke Inokuma[1], Satoru Aoyagi[1], Nao Saito[1], Maria Maroto Iitani[1], Erina Homma[1], Kokichi Hamasaka[2] and Hiroshi Shimizu[1]
[1]Department of Dermatology, Hokkaido University Graduate School of Medicine, N15 W7, Sapporo 060-8638, and [2]Hamasaka Skin Clinic, Sapporo, Japan. E-mail: inokuma@med.hokudai.ac.jp
Accepted June 2, 2009.

Sir,

Bowen's disease (BD) is one of the most common premalignant conditions of the skin. It can occur at any location on the body, presenting as a reddish plaque with scales. Rare cases of presentation as lesions on the nail unit with longitudinal melanonychia have also been described (2). Trauma, exposure to radiation, and intake of arsenic have been cited as causative factors of BD (1, 2). Recently human papillomavirus (HPV), in most cases HPV type 16, has been implicated as another causal agent of BD (1). We report here a case of BD presenting as melanonychia on the nail matrix detected as HPV type 56 (HPV-56) (2, 3).

CASE REPORT

A previously healthy 41-year-old Japanese man presented with a 2-mm-wide black streak on the nail and a 2-mm-wide, hyperkeratotic black macule on the lateral nail fold of the right index finger, which had been present for more than 2 years (Fig. 1). The Hutchinson sign was not present. There was no evidence of viral warts anywhere, including on the hands, feet and genital region, and no dark streaks in the nails of his other digits. Dermoscopic examination of the nail plate revealed longitudinal black pigmentation with parallel regular lines. Dermoscopic findings around the nail revealed homogenous black pigmentation and hyperkeratosis without vessels. A longitudinal excisional biopsy of the nail bed and the proximal and lateral nail fold was performed. Histopathological findings revealed acanthotic epidermis with atypical dyskeratotic keratinocytes (Fig. 2a). The nuclei of the atypical cells were large, pleomorphic, hyperchromatic, and bizarre mitotic. Many granules of melanin were seen in the nail plate and the epidermis of the nail bed without increases in the number of melanocytes (Fig. 2b). The papillary dermis was not involved in the malignant process. A diagnosis of BD was made. Polymerase chain reaction (PCR) amplification for DNA of HPV-6, 11, 16, 18, 30, 31, 33, 35, 39, 45, 51, 52, 56, 59, and 66 from the tissue of the lesion was positive only for HPV-56.

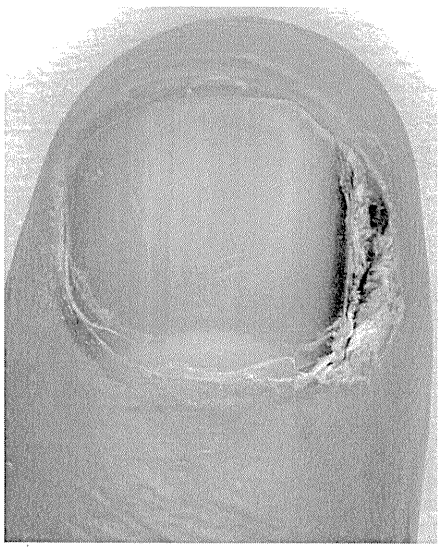

Fig. 1. A black streak on the nail and hyperkeratotic black macule on the lateral nail fold of the right index finger.

DISCUSSION

In most cases of BD with HPV, the lesions present as black papules in the genital region or as melanonychia, and the HPV detected from the lesion is typically HPV-16 (1). However, there is no information on the skin phototypes of people involved in these cases. In recent studies, however, HPV-56 has rarely been identified from BD lesions. HPV-56 was first detected from cervical intraepithelial neoplasia in 1989 (4); since then, it has frequently been detected in cervical neoplasia, in contrast to the low incidence of detection in normal cervical tissues and condylomas. At present, HPV-56 is included in the high-risk group or the mucous membrane group. In 1999, the first case of BD in an extra-genital area in which HPV-56 was detected was reported (5), and in 2003 the first case of detection of HPV-56 in the nail matrix with BD was reported (2). Since then, only two other similar cases have been reported (3). In all of these cases, the clinical features showed regular pigmented streaks and histopathological findings revealed many granules of melanin and atypical keratinocytes with large, hyperchromatic and bizarre mitotic nuclei.

In our case there were no control samples from matched locations in the same individual and, to the best of our knowledge, in others where HPV-56 has been found, there have been no control samples. In other patients with BD we examined who had no pigmentation, we did not detect HPV-56.

 doi: 10.2340/00015555-0723
 ISSN 0001-5555

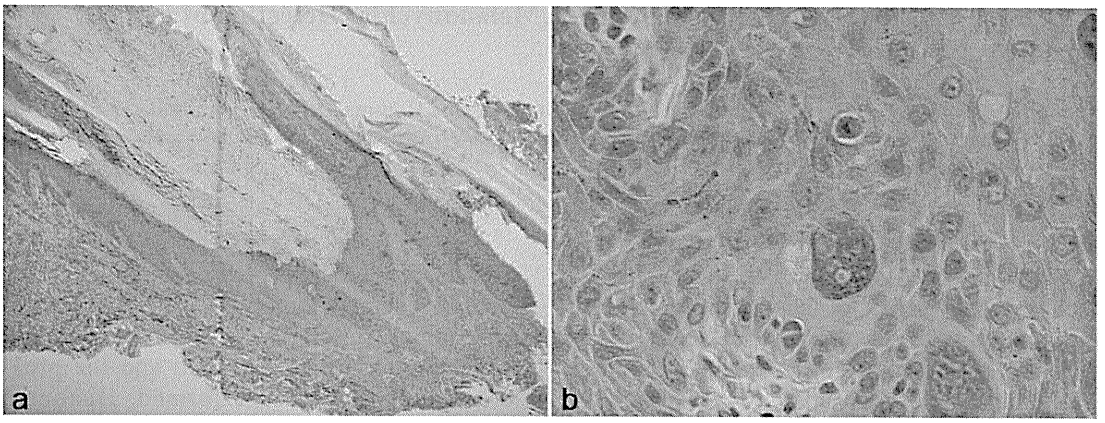

Fig. 2. (a) Acanthotic epidermis with dyskeratotic and atypical keratinocytes. (b) Large, pleomorphic, hyperchromatic, bizarre mitotic nuclei of atypical keratinocytes. Many melanin granules are seen in the nail plate and the epidermis of the nail bed. Haematoxylin and eosin (H&E) stain (a: ×40, b: ×400).

We hypothesize that HPV-56 is not only associated with the pathomechanism of carcinogenesis in BD, but that it is also a causative factor of pigmentation in this disease.

The authors declare no conflict of interest.

REFERENCES

1. McHugh RW, Hazen P, Eliezri YD, Nuovo GJ. Metastatic periungual squamous cell carcinoma: detection of human papillomavirus type 35 RNA in the digital tumor and axillary lymph node metastases. J Am Acad Dermatol 1996; 34: 1080–1082.
2. Lambiase MC, Gardner TL, Altman CE, Albertini JG. Bowen disease of the nail bed presenting as longitudinal melanonychia: detection of human papillomavirus type 56 DNA. Cutis 2003; 72: 305–309; quiz 296.
3. Shimizu A, Tamura A, Abe M, Motegi S, Nagai Y, Ishikawa O, et al. Detection of human papillomavirus type 56 in Bowen's disease involving the nail matrix. Br J Dermatol 2008; 158: 1273–1279.
4. Lorincz AT, Quinn AP, Goldsborough MD, McAllister P, Temple GF. Human papillomavirus type 56: a new virus detected in cervical cancers. J Gen Virol 1989; 70: 3099–3104.
5. Uezato H, Hagiwara K, Ramuzi ST, Khaskhely NM, Nagata T, Nagamine Y, et al. Detection of human papilloma virus type 56 in extragenital Bowen's disease. Acta Derm Venereol 1999; 79: 311–313.

suggest that the SNP had no influence on the C5 synthesis. Similar analyses in RA patients are needed to confirm this observation.

In this study, the lack of association of the SNP G/A (rs10818488) with pemphigus emphasizes the dilemma concerning the contribution of complement in pemphigus pathogenesis.

In fact, complement was described as an effective mediator in many studies based on cell culture detachment in the presence or absence of complement.[2] However, extensive erosions were obtained in C5-deficient mice suggesting that acantholysis could be complement independent.[9]

Further studies are needed to clarify if this polymorphism is restricted to RA or associated with other autoimmune diseases, where complement has a crucial role in disease pathogenesis, such as systemic lupus erythematosus.[10] Evaluating the association of other SNPs in the *TRAF1/C5* region will be needed to clarify their effect on the signalling cascade and to elucidate their involvement in autoimmune diseases.

Acknowledgments

The study was supported by grants from CMCU (Comité Mixte de Coopération Universitaire franco-tunisienne). This work was also supported by L'Association Française des Polyarthritiques, Société Française de Rhumatologie, Association Rhumatisme et Travail, Association Polyarctique, Groupe Taitbout, Académie de Médecine, Association de Recherche sur la Polyarthrite, Genopole, Conseil Régional Ile de France, Fondation pour la Recherche Médicale, Université Evry-Val d'Essonne, European Union for AutoCure and unrestricted institutional support from Wyeth, Schering-Plough, Pfizer and Amgen. We would like to thank Mr Paul Cant for reviewing the manuscript.

Laboratoire d'Immunologie, Hôpital la Rabta, Tunis, Tunisia — K. Mejri, H. Mbarek*
**Genhotel-EA3886, Evry & Paris 7 Universities, AP-HP and CHSF Hospitals, AutoCure European Consortium member, 91057 Evry-Genopole, France* — M. Kallel-Sellami, E. Petit-Teixeira*, Y. Zerzeri
†Laboratoire d'Immunologie, Hôpital Habib Bourguiba, Sfax, Tunisia — O. Abida†, M. Zitouni, M. Ben Ayed†
‡Service de Dermatologie, Hôpital la Rabta, Tunis, Tunisia — M. Mokni‡
§Service de Dermatologie, Hôpital Charles Nicolle, Tunis, Tunisia — B. Fezza§, H. Turki¶
¶Service de Dermatologie, Hôpital Hédi Chaker, Sfax, Tunisia — F. Tron**, D. Gilbert**, H. Masmoudi†
***INSERM U519, Institut Fédératif de Recherche Multidisciplinaire sur les Peptides (IFR23), Faculté Mixte de Médecine et de Pharmacie, Rouen, France* — B. Prum††, F. Cornelis*, S. Makni
††Laboratoire Statistique et Génome, Evry, France
Correspondence: Sondes Makni.
E-mail: sondes.makni@rns.tn

References

1 Tron F, Gilbert D, Joly P *et al.* Immunogenetics of pemphigus: an update. *Autoimmunity* 2006; **39**:1–9.
2 Kawana S, Geoghegan WD, Jordon RE. Complement fixation by pemphigus antibody II. Complement enhanced detachment of epidermal cells. *Clin Exp Immunol* 1985; **61**:517–25.
3 Plenge RM, Seielstad M, Padyukov L *et al.* TRAF1-C5 as a risk locus for rheumatoid arthritis—a genomewide study. *N Engl J Med* 2007; **357**:1199–209.
4 Kurreeman FA, Padyukov L, Marques RB *et al.* A candidate gene approach identifies the TRAF1/C5 region as a risk factor for rheumatoid arthritis. *PLoS Med* 2007; **4**:e278.
5 Bastuji-Garin S, Souissi R, Blum L *et al.* Comparative epidemiology of pemphigus in Tunisia and France: unusual incidence of pemphigus foliaceus in young Tunisian women. *J Invest Dermatol* 1995; **104**:302–5.
6 Dragon-Durey MA, Fremeaux-Bacchi V, Blouin J *et al.* Restricted genetic defects underlie human C6 deficiency. *Clin Exp Immunol* 2003; **132**:87–91.
7 Jenicek M, Cléroux R. *Epidémiologie: Principes, Techniques, Applications*, Québec edn. St-Hyacinthe: Edisem, 1982.
8 Kurreeman FA, Rocha D, Houwing-Duistermaat J *et al.* European Consortium on Rheumatoid Arthritis Families. Replication of the tumor necrosis factor receptor-associated factor 1/complement component 5 region as a susceptibility locus for rheumatoid arthritis in a European family-based study. *Arthritis Rheum* 2008; **58**:2670–4.
9 Anhalt GJ, Till GO, Diaz LA *et al.* Defining the role of complement in experimental pemphigus vulgaris in mice. *J Immunol* 1986; **137**:2835–40.
10 Atkinson JP. Complement system on the attack in autoimmunity. *J Clin Invest* 2003; **112**:1639–41.

Key words: *complement C5, desmoglein, pemphigus, single-nucleotide polymorphism (SNP)*

Conflicts of interest: none declared.

Birt–Hogg–Dubé syndrome with clear-cell and oncocytic renal tumour and trichoblastoma associated with a novel *FLCN* mutation

DOI: 10.1111/j.1365-2133.2009.09134.x

Sir, Birt–Hogg–Dubé (BHD) syndrome is a rare autosomal dominant syndrome characterized by skin hamartomas and multiple renal tumours.[1,2] *FLCN* (previously known as BHD) is the responsible gene, encoding a folliculin, which is suspected to be a tumour suppressor.[3] We report here a case of a Japanese patient with BHD syndrome with a new mutation in exon 12 of the *FLCN* gene, manifesting a trichoblastoma on the scalp and a renal tumour with atypical histological features.

A 68-year-old Japanese man was transferred to our hospital for further treatment of a cerebral infarction. From his early years he had had copious papules all over his face and neck. His mother and sister died from unknown renal disease. The patient's son also had similar papules since his early years. The patient's daughter had no such lesions. There was an 18 × 19 × 9 mm, dome-shaped, smooth-surfaced, greyish,

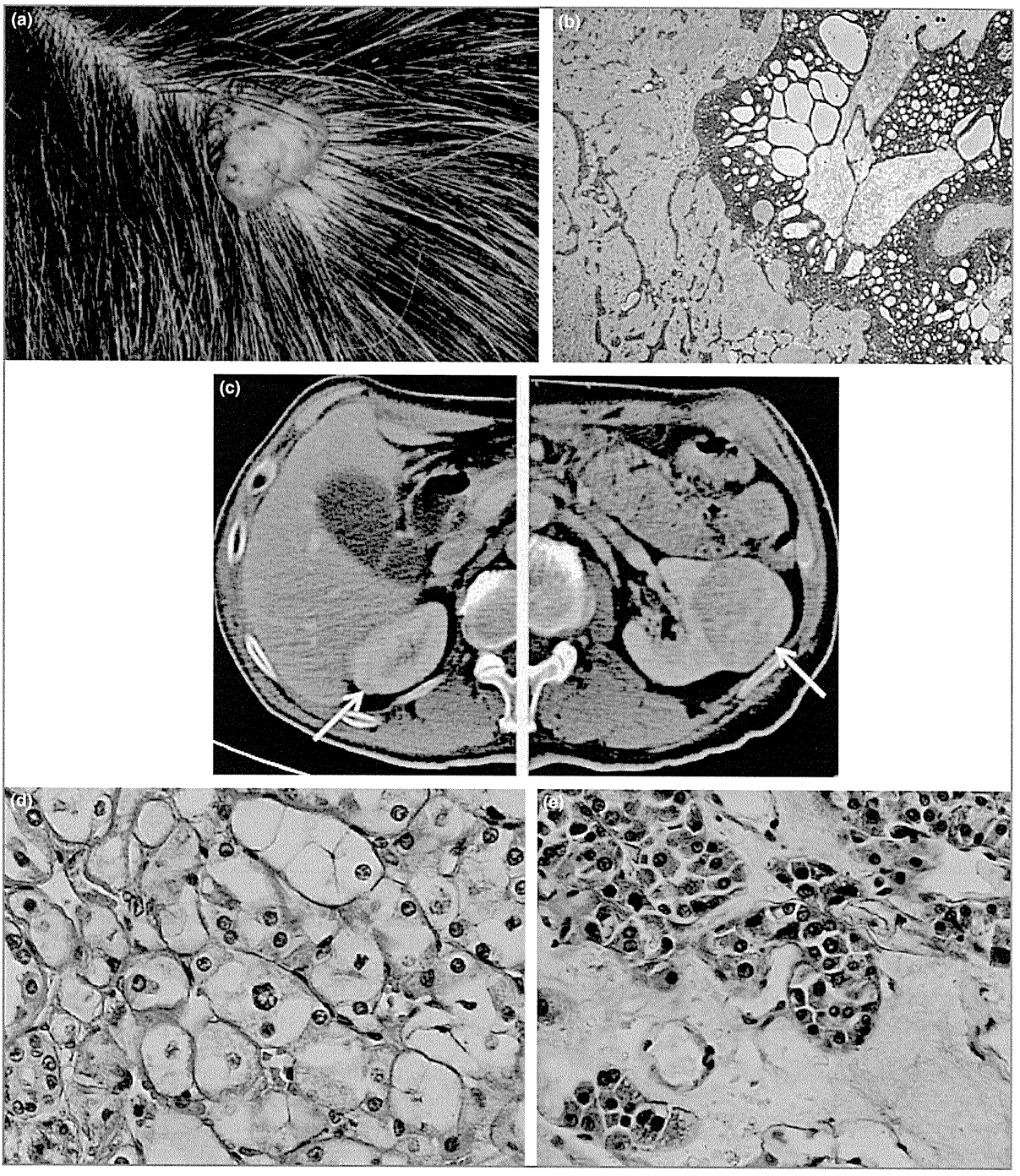

Fig 1. (a) A tumour on the patient's right parietal region. (b) A specimen from the tumour showed that the lesion was composed of multiple nodules of basaloid cells arranged in a cribriform pattern with peripheral palisading, partly with follicular differentiation. In contrast to the pattern of basal cell carcinoma, there was no cleft between tumour and stroma. (c) Computed tomography scans of the patient's abdomen revealed bilateral renal tumours (arrows). (d, e) Pathology of the renal cell carcinoma. The tumour was mainly composed of cells with clear to acidophilic cytoplasm arranged in alveolar, tubular and focal papillary fashion, indicating conventional (clear-cell) carcinoma of the kidney (d). Focal oncocytic areas were also observed in which round to oval tumour cells with granular acidophilic cytoplasm were organized into various-sized nests within a loose fibrous stroma. The nuclei in the oncocytic area were uniform and round, with or without prominent nucleoli (e).

firm, hairless tumour on his right parietal region (Fig. 1a). We obtained a biopsy specimen from one of the facial papules and surgically excised the tumour on the head. A specimen from a facial papule showed a typical feature of fibrofolliculoma. Specimens from the parietal tumour showed that the lesion was composed of multiple nodules of basaloid cells

arranged in a cribriform pattern with peripheral palisading, partly with follicular differentiation (Fig. 1b). We finally diagnosed this tumour as a trichoblastoma.

Computed tomography scans showed no pulmonary lesion, but identified two enhanced heterogeneous masses in the bilateral kidneys, the larger one (50 mm) was in the middle portion of the left kidney, and the smaller one (5 mm) was in the upper pole of the right kidney. The tumours were enhanced in dynamic early phase and washed out in dynamic parenchymal phase. These findings were consistent with renal cell carcinoma. Further imaging studies detected no lymphadenopathy or metastasis, and the clinical diagnosis was left renal cell carcinoma, T1bN0M0 and right renal cell carcinoma, T1aN0M0 (Union Internationale Contre Cancrum) (Fig. 1c). Initially, a laparoscopic left radical nephrectomy was performed, because the tumour was very close to the renal pelvis and partial nephrectomy was technically difficult. Macroscopically, the tumour in the left kidney was 50 mm in diameter with a fibrous capsule and a mahogany-brown colour of its cut surface with no haemorrhage or necrosis. A histopathological examination revealed that the tumour was mainly composed of cells with clear to acidophilic cytoplasm arranged in alveolar, tubular and focal papillary fashion, indicating clear-cell carcinoma of the kidney (Fig. 1d). Focal oncocytic areas were also observed in which round to oval tumour cells with granular acidophilic cytoplasm were organized into various-sized nests within a loose fibrous stroma. The nuclei in the oncocytic area were uniform and round, with or without prominent nucleoli (Fig. 1e). Immunohistochemically, the tumour cells in the clear-cell carcinoma area were positive for vimentin, but the tumour cells in the oncocytic area were negative for vimentin (not shown). This feature is compatible with oncocytoma. Neither capsular nor vascular invasion was seen. The right-side tumour has been followed by imaging without therapy.

Total genomic DNA was extracted from the patient's peripheral blood leucocytes, and the segments of the *FLCN* gene including all exons (4–14) were amplified and directly sequenced. This mutation analysis finally detected a duplication of 7 bp (GTTCCAC) at codon 448 (c.1792–1798) in exon 12 (Fig. 2). There was no similar mutation reported in the Human Gene Mutational Database; therefore we suggest that this is a novel mutation in the *FLCN* gene. No mutation was detected in exon 11, a hot spot in previous mutation analyses in Caucasian and Asian patients.[4,5] This insertion led to a premature termination codon 33 bp downstream from the site of insertion. The patient's daughter did not have this mutation (not shown). Consent for gene analysis of his other family members, including his son was not obtained.

This is the first reported case of a patient with BHD syndrome with trichoblastoma, not basal cell carcinoma.[6] The kidney tumour consisted mainly of clear-cell carcinoma, with oncocytoma and papillary renal cell carcinoma. The histological features were distinctly unusual and were different from those of a hybrid oncocytic tumour, the most common renal cell carcinoma in BHD syndrome, although clear-cell carcinoma is part of the tumour spectrum.[7] A few cases of other

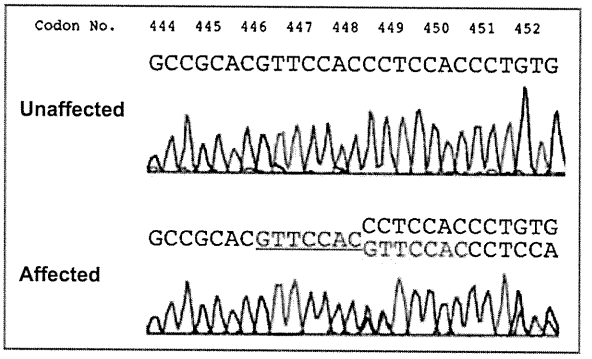

Fig 2. Detection of a mutation in codon 448 (c.1792–1798dupGTTCCAC) in exon 12, a repeat of the preceding 7 bp in one allele, resulting in unclear multiple chromatograms after the tract.

mutations in exon 12 have been reported previously. However, these cases do not seem to share apparent common clinical features.[6,8–10] There have been no reports of sporadic trichoblastoma or basal cell carcinoma with mutations in the *FLCN* gene. Further research is required to define the protein structure and reveal its functionally active sites.

This case suggests that BHD syndrome is associated with a variety of cutaneous hamartomas including trichoblastoma. A new mutation in the present case of BHD syndrome may be a crucial event in follicular differentiation and renal carcinogenesis.

Acknowledgment

We thank Dr Takahiro Hamada, Department of Dermatology, Kurume University School of Medicine, for his helpful suggestions.

Department of Urology, Graduate School of Medical Sciences, Kyushu University, Fukuoka, Japan — K. Imada
**Department of Dermatology, Kurume University School of Medicine, 67 Asahimachi, Kurume, Fukuoka 830-0011, Japan* — T. Dainichi*, A. Yokomizo, T. Tsunoda
†Department of Anatomic Pathology, Graduate School of Medical Sciences, Kyushu University, Fukuoka, Japan — Y.H. Song†
‡Department of Dermatology, Hokkaido University Graduate School of Medical Sciences, Sapporo, Japan — A. Nagasaki‡, H. Shimizu‡, T. Hashimoto*
§Department of Dermatology, Hirosaki University School of Medicine, Hirosaki, Japan — D. Sawamura§
¶Department of Dermatology, Graduate School of Medical Sciences, Kyushu University, Fukuoka, Japan — W. Nishie‡, S. Fukagawa¶, K. Urabe¶, M. Furue¶, S. Naito
Correspondence: Teruki Dainichi.
E-mail: dainichi@med.kurume-u.ac.jp

References

1 Birt AR, Hogg GR, Dubé WJ. Multiple fibrofolliculomas with trichodiscomas and acrochordons. *Arch Dermatol* 1977; **113**:1674–7.

2 Toro JR, Glenn G, Duray P *et al.* Birt–Hogg–Dubé syndrome: a novel marker of kidney neoplasia. *Arch Dermatol* 1999; **135**:1195–202.

3 Nickerson ML, Warren MB, Toro JR *et al.* Mutations in a novel gene lead to kidney tumors, lung wall defects, and benign tumors of the hair follicle in patients with the Birt–Hogg–Dubé syndrome. *Cancer Cell* 2002; **2**:157–64.

4 Kawasaki H, Sawamura D, Nakazawa H *et al.* Detection of 1733insC mutations in an Asian family with Birt–Hogg–Dubé syndrome. *Br J Dermatol* 2005; **152**:142–5.

5 Schmidt LS, Nickerson ML, Warren MB *et al.* Germline BHD-mutation spectrum and phenotype analysis of a large cohort of families with Birt–Hogg–Dubé syndrome. *Am J Hum Genet* 2005; **76**:1023–33.

6 Toro JR, Wei M-H, Glenn GM *et al.* BHD mutations, clinical and molecular genetic investigations of Birt–Hogg–Dubé syndrome: a new series of 50 families and a review of published reports. *J Med Genet* 2008; **45**:321–31.

7 Pavlovich CP, Grubb RL 3rd, Hurley K *et al.* Evaluation and management of renal tumors in the Birt–Hogg–Dubé syndrome. *J Urol* 2005; **173**:1482–6.

8 Gunji Y, Akiyoshi T, Sato T *et al.* Mutations of the Birt Hogg Dubé gene in patients with multiple lung cysts and recurrent pneumothorax. *J Med Genet* 2007; **44**:588–93.

9 Leter EM, Koopmans AK, Gille JJ *et al.* Birt–Hogg–Dubé syndrome: clinical and genetic studies of 20 families. *J Invest Dermatol* 2008; **128**:45–9.

10 van Steensel MA, Verstraeten VL, Frank J *et al.* Novel mutations in the BHD gene and absence of loss of heterozygosity in fibrofolliculomas of Birt–Hogg–Dubé patients. *J Invest Dermatol* 2007; **127**:588–93.

Key words: *Birt–Hogg–Dubé syndrome, mutation, oncocytoma, renal cell carcinoma, trichoblastoma*

Conflicts of interest: none declared.

LEF-1 expression in basal cell carcinomas

DOI: 10.1111/j.1365-2133.2009.09144.x

SIR, Basal cell carcinomas (BCCs) are the most frequent tumours of the skin, and are thought to arise from stem

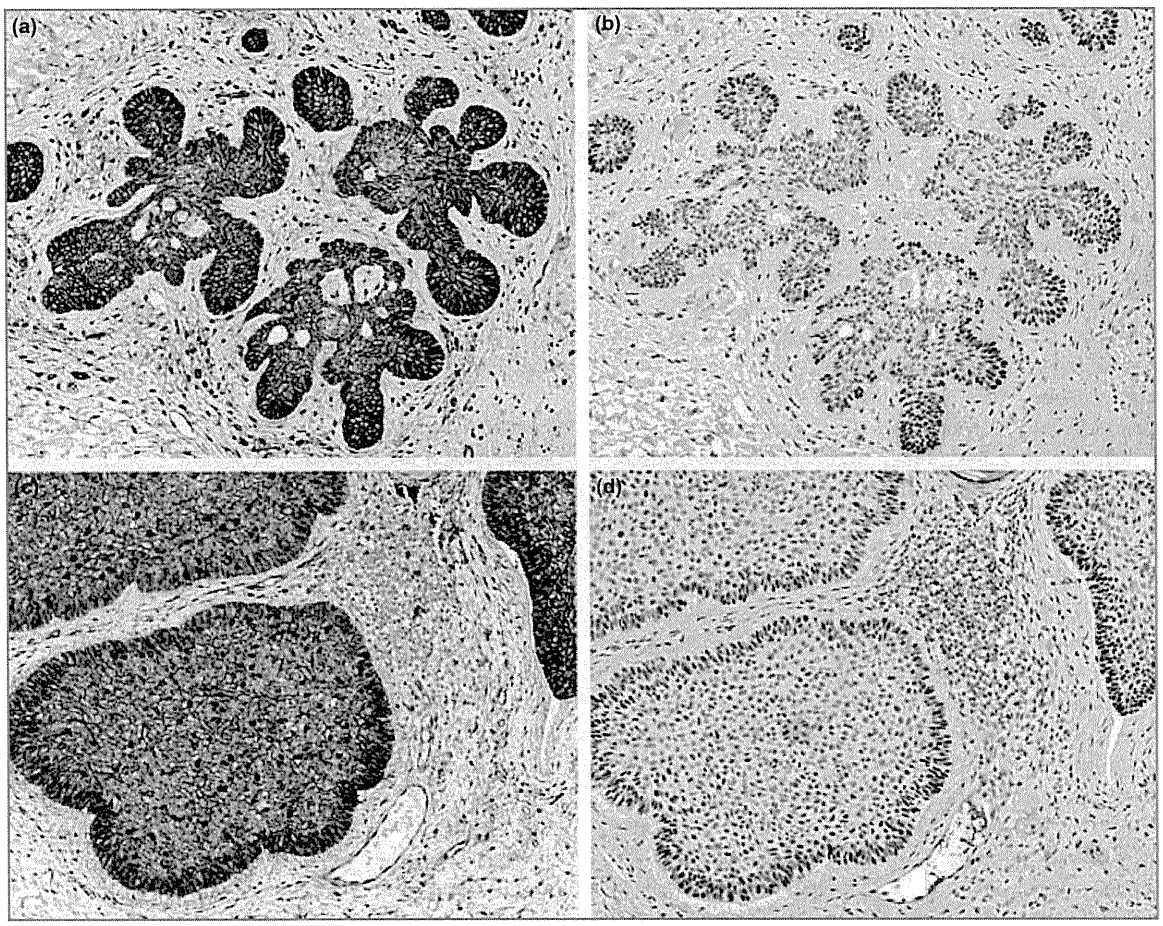

Fig 1. β-catenin and LEF-1 expression patterns. Two patterns of β-catenin and LEF-1 expression were distinguishable in basal cell carcinoma. (a, b) The invasive pattern of β-catenin (a) and LEF-1 (b) displayed an intense nuclear staining of the cells at the invasive margins and an absent nuclear staining of the cells in the tumour centre. (c, d) The diffuse pattern exhibited positive nuclear β-catenin (c) and LEF-1 (d) tumour cells on the periphery and positive cells in the tumour centre. Original magnification: (a–d) × 200.

CONCISE COMMUNICATION

BJD British Journal of Dermatology

Analysis of Taiwanese ichthyosis vulgaris families further demonstrates differences in *FLG* mutations between European and Asian populations

C-K. Hsu,*†‡ M. Akiyama,* I. Nemoto-Hasebe,* T. Nomura,*§ A. Sandilands,§ S-C. Chao,† J.Y-Y. Lee,† H-M. Sheu,† W.H.I. McLean§ and H. Shimizu*

*Department of Dermatology, Hokkaido University Graduate School of Medicine, North 15 West 7, Kita-ku, Sapporo 060-8638, Japan
†Department of Dermatology and ‡Institute of Clinical Medicine, College of Medicine, National Cheng Kung University Hospital, Tainan, Taiwan
§Epithelial Genetics Group, Division of Molecular Medicine, University of Dundee, Colleges of Life Sciences and Medicine, Dentistry and Nursing, Dundee, U.K.

Correspondence
Masashi Akiyama.
E-mail: akiyama@med.hokudai.ac.jp

Accepted for publication
24 December 2008

Key words
atopic eczema, filaggrin, FLG, ichthyosis, mutation

Conflicts of interest
W.H.I.M. has filed patents relating to genetic testing and therapy development aimed at the filaggrin gene.

DOI 10.1111/j.1365-2133.2009.09112.x

Summary

Background Mutations in the gene encoding filaggrin (FLG) were identified to underlie ichthyosis vulgaris (IV) and also shown to predispose to atopic eczema. Until now, no *FLG* mutations have been described in the Taiwanese population.
Objectives To elucidate filaggrin mutations in the Taiwanese population and further to clarify the population genetics of filaggrin gene mutations in the Asian populations.
Methods In the present study, 12 individuals from four unrelated Taiwanese IV families were examined for *FLG* mutations. We carried out comprehensive sequencing of the entire *FLG* coding region using an overlapping polymerase chain reaction strategy.
Results We identified three *FLG* mutations in the Taiwanese IV families. One mutation E1795X was a previously unidentified *FLG* mutation, which might be specific to the Taiwanese. Interestingly, another *FLG* mutation 3321delA is prevalent in the Japanese population and the other mutation Q2417X was found in the Singaporean Chinese population. No *FLG* mutation identified in the white European population was found in the Taiwanese population.
Conclusions The present findings suggest that the Taiwanese population, as an East Asian group, share *FLG* mutations with both the Japanese and the Singaporean Chinese population. In addition, these results exemplify differences in the population genetics of filaggrin between Europe and Asia.

Ichthyosis vulgaris (IV; OMIM 146700) is a common inherited skin disorder exhibiting scaling and dry skin that is particularly prominent on the extensor surfaces of limbs and the lower abdomen, and is associated with palmoplantar hyperlinearity.[1–3] Histologically, IV is characterized by a decrease in the size and number or complete absence of keratohyaline granules in the upper epidermis.[1] Loss-of-function mutations in the profilaggrin/filaggrin gene (*FLG*) which resides within the epidermal differentiation complex on chromosome 1q21 have been identified as the cause of IV.[2] After establishment of sequencing methods for the entire *FLG* coding region,[4] 22 nonsense or frameshift mutations in *FLG* have been reported to date.[5] Most *FLG* mutations are specific to particular ancestral groups, such as the white European,[4] Japanese[6,7] and Singaporean Chinese populations.[8]

In this study, we identified three *FLG* mutations in Taiwanese IV families. One mutation E1795X was a previously unidentified *FLG* mutation which might be specific to the Taiwanese population. The other two mutations were recurrent mutations previously identified in the Japanese or the Singaporean Chinese population, but not in the white European population. These results exemplify differences in the population genetics of filaggrin between Europe and Asia.

Materials and methods

Patients

In total, 12 individuals from four unrelated Taiwanese IV families, designated families 1–4, were examined for *FLG* mutations (Fig. 1). The diagnosis of IV was established from clinical features of variable scaling on the extremities, dry skin, palmoplantar hyperlinearity, early onset and a positive family history. These Taiwanese families had no traceable Japanese or

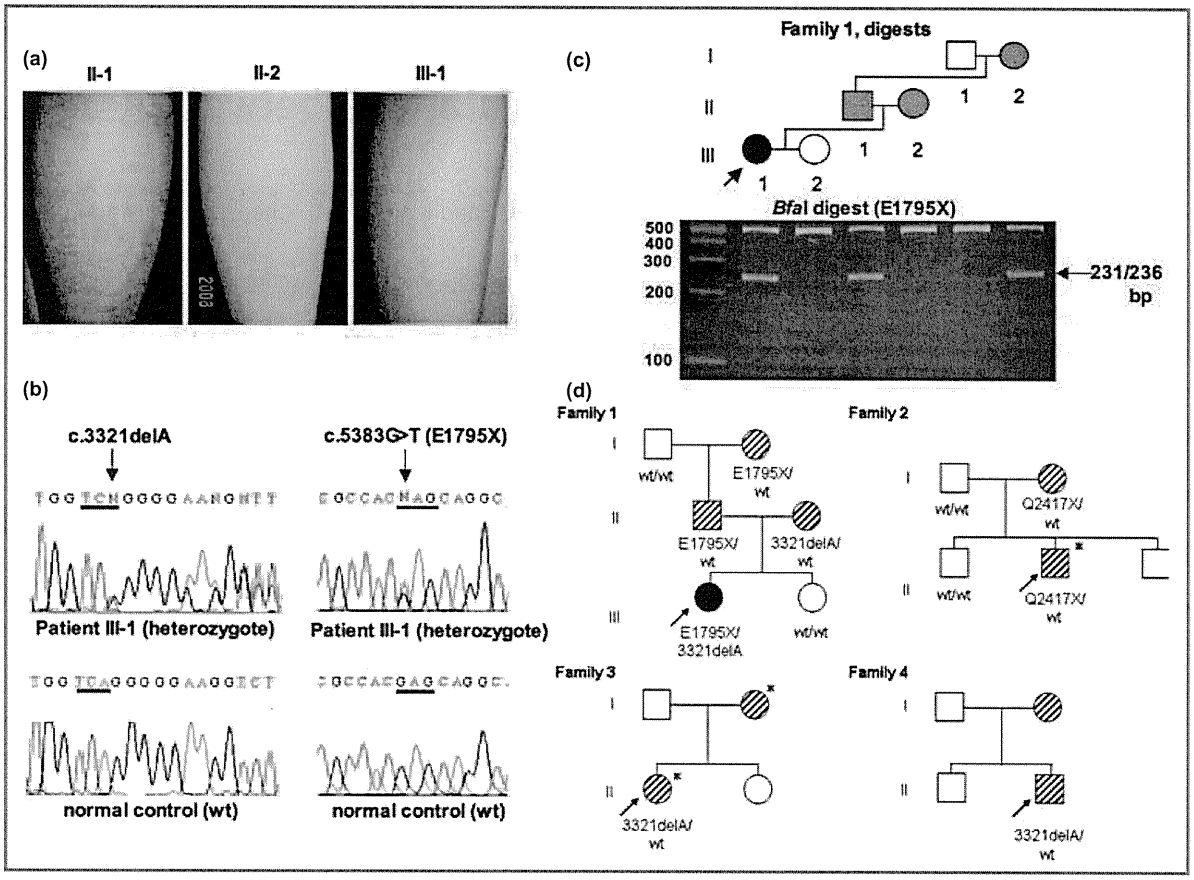

Fig 1. *FLG* mutations in Taiwanese ichthyosis vulgaris (IV) families. (a) Fine scaling on the patients with IV in family 1. The proband (III-1) showed a more severe IV phenotype than her father (II-1) and mother (II-2). (b) The proband of family 1 was a compound heterozygote for a deletion mutation c.3321delA and a previously unidentified nonsense mutation c.5383G>T (E1795X). (c) Verification of the mutation E1795X by BfaI restriction enzyme digestion: 467-bp fragments amplified from the mutant alleles are digested into 236-bp and 231-bp fragments, whereas those from wild-type alleles are uncut. The polymerase chain reaction products from I-2, II-1 and III-1 (heterozygotes for E1795X) revealed two bands, 467-bp and 236-bp/231-bp bands, because 236-bp and 231-bp products were detected as one overlapping band in this gel electrophoresis. I-1, II-2 and III-2 had only wild-type alleles. (d) Family trees and *FLG* mutations in the IV families studied. Solid symbols refer to the marked IV presentation; cross-hatched symbols refer to the milder IV presentation. In addition, three of 10 patients with IV had concomitant dermatologist-diagnosed atopic eczema (*). wt, wild-type for *FLG* mutations.

European ancestry, and they were all from the southeast coast of China. We performed a skin biopsy from the upper left arm of the proband in family 4. Light microscopy and immunohistochemical staining were performed as previously described[6] and showed mild hyperkeratosis with a marked reduction in epidermal filaggrin expression compared with healthy individuals.

Mutation detection

Genomic DNA samples from peripheral blood cells of the patients and their family members were analysed for filaggrin mutations. The medical ethical committee at Hokkaido University Graduate School of Medicine and the Human Experiment and Ethics Committee of National Cheng Kung University Hospital approved all the studies. The study was conducted according to the Declaration of Helsinki Principles. Participants or their legal guardians gave their written, informed consent.

All samples from the four IV families were screened for the six previously reported Japanese-specific mutations (3321delA, S1695X, Q1701X, S2554X, S2889X and S3296X),[6,7,9] as well as the six mutations found in Singaporean Chinese (441delA, 1249insG, Q2417X, E2422X, 7945delA and R4307X).[8] *FLG* mutations were studied by direct sequencing, fluorescent polymerase chain reaction (PCR) and/or enzyme digestion assays as described previously.

To identify further mutations, we carried out comprehensive sequencing of the *FLG* gene using an overlapping PCR strategy that allows routine diagnostic sequencing of the entire filaggrin coding sequence.[4]

Results

We identified two recurrent mutations: 3321delA, previously reported in the Japanese population, in three families (families

